

Purification of Oleylamine for Materials Synthesis and Spectroscopic Diagnostics for *trans* Isomers

Dmitry Baranov,[#] Michael J. Lynch,[†] Anna C. Curtis,[‡] Alexa R. Carollo, Callum R. Douglass,
Alina M. Mateo-Tejada, and David M. Jonas*

Department of Chemistry, University of Colorado, 215 UCB, Boulder, Colorado 80309, USA

[#]Present address: Italian Institute of Technology, Genoa, 16163, Italy

*[†]Present address: Department of Chemistry, University of Minnesota, Minneapolis, Minnesota,
55455, USA*

[‡]Present address: Department of Chemistry, Radford University, Radford, Virginia, 24142, USA

Contents

1) Additional notes on the experimental procedure for purification of commercial oleylamine reagents.	3
2) Experimental characterization procedures	5
2.1) ^1H NMR.....	5
2.2) FTIR.....	7
2.3) Elemental analysis	7
2.4) Mass spectrometry	7
2.5) Raman spectroscopy	8
3) Test for peroxides in as-received and purified oleylamine	9
4) ATR-IR test for carbamates	10
5) Precipitation Tests for Lead Chloride and Sulfur with Acetonitrile Non-Solvent.....	15
6) Lead Sulfide Quantum Dot Synthesis	16
7) Tables of proton integrals.....	21
8) Mass spectra	24
9) Table of mass spectra peaks	25
10) UV-Vis absorbance spectra before and after purification	26
11) Table of elemental analyses	27
12) Ratio method as applied to ^1H NMR, Raman, and FTIR spectra.....	28
12.1) ^1H NMR	28
12.2) Raman	30
12.3) FTIR.....	31
13) FTIR spectra.....	33
14) ^1H NMR spectra	36
15) References	52

1) Additional notes on the experimental procedure for purification of commercial oleylamine reagents.

The purification procedure described in the main text was used for all studies of lead chloride in oleylamine described in the main text. The additional observations and modifications below were used for studies of lead bromide and lead iodide solubility in oleylamine. As a control, these same tests were performed on lead chloride using the modifications below. We were unable to establish a reproducible difference between the solubility of lead chloride in 70% technical grade (3.7:1 *cis-trans* ratio) and 98% primary amine (1.1:1 *cis-trans* ratio) oleylamine reagents that had been purified, dried, and filtered. Other tests described in the main text were not performed using these modifications of the oleylamine purification procedure. All steps of the purification were done in a fume hood.

a) Conversion of oleylamine reagent to oleylamine hydrochloride:

HCl was added to the oleylamine and ether solution dropwise using a separatory funnel at a rate of 1 drop every 3-5 seconds. A 1" stir bar spinning quickly enough to form a deep vortex in the oleylamine flask ensured a rapid and uniform distribution of the acid. The oleylamine solution was maintained at room temperature in a 600 mL water bath at ~20 °C.

b) Filtration and drying:

After the oleylamine solution was added dropwise to the acetonitrile, the resultant oleylamine hydrochloride solid was pale yellow (70% technical grade, Aldrich, Lot # STBD9442V) or white with a slight hint of pink or orange ($\geq 98\%$ primary amine, Aldrich, Lot # MKBZ7016V). The color persisted through the washing steps. Several successful purification batches were performed without the vacuum drying step listed in the main text.

c) Separation of phases following sodium hydroxide addition:

During some successful purifications, slow (several hours) separation of the aqueous and organic phases was observed.

d) Use and removal of drying agent:

Sodium sulfate (~20g) was used to dry the organic phase for two hours prior to distillation.¹ The sulfate was removed via gravity filtration through Whatman 2 filter paper (Cat No. 1002).

e) Removal of ether:

Ether was removed from the oleylamine solution by gently heating the solution in a ~50 °C oil bath while blowing dry nitrogen gas over the surface until no further volume change was observed.

f) Distillation:

The oleylamine was placed in round a bottom flask with ~1.5 cm³ of freshly cut sodium metal and a stir bar. The flask and distillation apparatus were evacuated at a pressure of 25-50 mTorr for ~30 minutes prior to heating. The flask was immersed in an oil bath on a hot plate. The flask and distillation head were thoroughly wrapped with aluminum foil as insulation. The temperature of the oil bath was held between 175 and 185 °C throughout the distillation and the vapor temperature before the condensation jacket reached 140-150 °C (measured with an immersion thermometer). The vacuum pressure was held between 60 and 100 mTorr during the distillation and fell to 40 mTorr upon completion of distillation. The distillation typically took ~40 minutes once heating began. The oleylamine product of the distillation was clear and colorless in all successful purifications. The residue in the round bottom flask was yellow-orange with residual metallic sodium.

g) Yield:

For two purification batches using the procedure described above, the yield was measured to be 70-71%.

2) Experimental characterization procedures

2.1) ^1H NMR

Deuterated benzene (C_6D_6 , Cambridge Isotopes, 99.5%, DLM-1-25; benzene-d₆, prod.no. 561509-10X.75ML, Sigma-Aldrich, "100%", 99.96 atom %D, contains 0.03 % (v/v) TMS), deuterated dichloromethane (CD_2Cl_2 , Cambridge Isotopes, 99.8%, DLM-23-10; dichloromethane-d₂, prod.no. 444324-10X0.6ML, Sigma-Aldrich, 99.9 atom %D), deuterated cyclohexane (C_6D_{12} , Cambridge Isotopes, 99.5%, DLM-17-10X1), ferrocene [$\text{Fe}(\text{C}_5\text{H}_5)_2$, Strem, 99%, lot # 27479000, 99.7 wt.% assay by the manufacturer's certificate of analysis], air-tight NMR tubes (New Era, NE-HL5-ST-158), standard NMR tubes (New Era, NE-UL5-7). High purity oleic acid (*cis*-9-Octadecenoic acid, prod.no. O1008-25G, Sigma-Aldrich, $\geq 99\%$, lot # SLBH6395V) and elaidic acid (*trans*-9-Octadecenoic acid, prod.no. E4637-1G, Sigma-Aldrich, $\geq 99.0\%$, lot # SLBN7174V) were used as reference compounds for determination of chemical shifts of *cis*- and *trans*- vinylic and allylic protons in the hydrocarbon chain of the amine samples, and as reference compounds for testing the accuracy of integration for ^1H NMR spectra (see below). Both acids were stored in the dark, refrigerated, and handled inside the nitrogen-filled glovebox. The ^1H NMR spectra (32-64 scans, one second relaxation delay) were recorded on a Bruker Advance III 300 MHz instrument.

Samples of amine for ^1H NMR experiments were prepared by diluting a small amount of amine (20-60 μL) in ~ 0.6 ml of the deuterated solvent. Unpurified samples of amine were prepared in air using standard NMR tubes capped with a plastic cap. Samples of purified amine were handled inside the nitrogen-filled glovebox using dry deuterated solvents and air-tight NMR tubes. ^1H NMR spectra in C_6D_6 and CD_2Cl_2 , were referenced to the residual solvent signals (δ^{H} [C_6D_6] = 7.16 ppm, singlet; δ^{H} [CD_2Cl_2] = 5.32 ppm, 1:1:1 triplet).² ^1H NMR spectra

in C₆D₁₂ could not be referenced to the residual solvent signal (δ^H [C₆D₁₂] = 1.38 ppm, singlet)³ as it overlaps with a signal from methylene hydrogens in the amine, so a small amount of ferrocene was added to the solution of amine in C₆D₁₂ and the chemical shifts in the resulting spectra were referenced to that of ferrocene (δ^H [Fe(C₅H₅)₂] = 4.04 ppm in C₆D₁₂).⁴

The accuracy of the proton integrals in the ¹H NMR spectra was estimated by comparing ratios of the integrals for methyl, allylic, vinylic, methylene, β -methylene, α -methylene, and carboxylic protons in the spectra of high purity oleic and elaidic acids to the theoretical ratio. The results are shown in Table S1. Based on these results, an estimate of the relative number of protons in the hydrocarbon chain of the analyzed compounds is deemed accurate to within ~2-5% of the theoretical value. This accuracy is consistent with literature recommendations.⁵ Table S2 gives proton integrals for the three amine samples in various solvents. Part of the discussion about amine purity relies on ratios between various proton integrals and their combinations. Thus, the propagation of uncertainty associated with each proton integral needs to be considered to assess the usefulness of any particular proton integral ratio. For the uncertainty propagation, we assumed an independent error of $\pm 3.5\%$ (the average between min. 2% and max. 5% error in the oleic/elaidic acid hydrocarbon chain proton integrals) for each proton integral value and calculated an error for each ratio of integrals using the error propagation formulas for addition and division (Table S3).

Linear primary amines with a hydrocarbon chain differing from that of oleylamine by m methylene groups ($\Delta m = 1, 2, 3\dots$ means longer chain; $\Delta m = -1, -2, -3\dots$ means shorter chain) and containing a total of k double bonds (no conjugation) have methylene to amine proton ratios of: $[15 + \Delta m - 2 \times (k - 1)]$. These impurities lower the methylene to amine proton ratios below 15. Impurities with empirical formulas consistent with $(\Delta m, k)$ combinations of $(-4, 0)$, $(-2, 1)$,

(-2, 0), (-1, 0), and (0, 2) were observed in the mass spectra (Table S4) and can account for the lowered methylene to amine proton ratios.

2.2) FTIR

IR spectra were recorded using Thermo Nicolet Avatar 360 FTIR spectrometer by placing a drop (5-10 μ L) of the neat sample between two 1" diameter KBr disks. High purity oleic and elaidic acids (see chemicals specification in the ^1H NMR section above) were used as reference standards for identification of vibrational modes arising from *cis*- and *trans*- isomers, respectively, at the double bond in the hydrocarbon chain. All samples had their FTIR spectra collected as neat substances in the liquid state.

2.3) Elemental analysis

C, H, and N wt.% analysis was performed on neat samples by Robertson Microlit Laboratories (Ledgewood, NJ). Samples of purified amine were packed under nitrogen and handled in the glovebox for elemental analysis.

2.4) Mass spectrometry

High-resolution mass spectra of the oleylammonium chloride were recorded at the Mass Spectrometry Facility at the University of Colorado Boulder using a Waters Synapt G2 HDMS mass spectrometer with Quadrupole/Time of Flight (ToF) mass analyzer in positive ion electrospray ionization (ESI+) mode. The matching of the empirical formula and the isotope distribution to the observed peaks in the HRMS spectra was aided by an Isotope Distribution Calculator and Mass Spec Plotter tool (Scientific Instrument Services, Inc.) available online at no cost.⁶ Agreement with the isotopic distributions and a match within 0.003 m/z units between the

calculated and experimental m/z value for the proposed molecular formula was considered to be adequate support for that molecular formula to be indicative of the registered species.^{7, 8}

2.5) Raman spectroscopy

Raman spectra of oleylamine samples with 488 nm excitation were recorded in 90° geometry on a home-built setup using an argon ion laser (Ion Laser Technology 5500ASL-00, ~70 mW of CW power at 488 nm) as an excitation source and a spectrometer consisting of a spectrograph (Acton SpectraPro 300i) and CCD detector (LN2 cooled, back-illuminated, Roper Scientific) as detailed elsewhere.⁹ For all 488 nm experiments, ~1 ml of each amine sample was placed in an air-tight 1 cm pathlength quartz cuvette.

Raman spectra with 532 nm excitation were collected in a backscatter geometry on a Raman microscope (Horiba Scientific Jobin Yvon XploRa, ~16 mW power at 532 nm).⁹ The samples for 532 nm experiments were prepared by placing a small volume of the amine sample (10-20 μL) into a square borosilicate capillary (0.5 \pm 0.05 mm inner diameter, 10 cm length, part no. 8250-100, VitroCom) under inert atmosphere followed by sealing of both capillary ends with a capillary wax (prod.no. HR4-328, Hampton Research). The accuracy of absolute Raman shifts measured on this setup was checked against Raman shifts of solid 4-acetamidophenol (prepared in a similar capillary), following the recommendation of the ASTM standard no. E1840.¹⁰ The deviation of Raman lines recorded for the 4-acetamidophenol on this apparatus from the average values reported in the standard was in the range of ~0-0.6 cm^{-1} , depending on the line, which is within a standard deviation of the line positions specified in the standard.

3) Test for peroxides in as-received and purified oleylamine

Peroxide content in as-received and in purified and dried oleylamine samples (70% technical grade, Aldrich, Lot # STBD9442V; $\geq 98\%$ primary amine, Aldrich, Lot # MKBZ7016V) was tested with colorimetric test strips (Peroxide Test, method: colorimetric with test strips, MQuantTM, Lot # HC854138) that use a peroxidase enzyme. According to the manufacturer, these colorimetric test strips are designed for inorganic peroxides in aqueous or organic solvents. For all samples tested, the resulting color of the reaction zone on the test strip was white. On the color scale provided, the white reaction zone color is labeled “0 mg/L H₂O₂,” and the next scale, colored pale blue, is labeled “0.5 mg/L H₂O₂.” No hydroperoxides were detected.

4) ATR-IR test for carbamates

It has been reported that oleylamine reacts with carbon dioxide from the atmosphere, forming ammonium carbamates.¹¹ A study on the carbon dioxide absorption kinetics of powders of alkylamines of different chain lengths revealed that short chain alkylamines reached carbon dioxide absorption saturation quicker than long chain alkylamines.¹² Octadecylamine was reported to react with carbon dioxide under atmospheric conditions to form octadecylammonium octadecylcarbamate, reaching complete conversion (half of the octadecylamine molecules formed octadecylammonium, and the other half formed octadecylcarbamate) after 940 hours of exposure.¹² The formation of some ammonium carbamates has been reported to be reversible upon heating.^{12, 13}

Ammonium carbamate formation in purified and dried oleylamine ($\geq 98\%$ primary amine, Aldrich, Lot # MKBZ7016V) was investigated. A 4 mL volume of purified and dried oleylamine was transferred into a quartz cuvette and closed with a rubber septum in the glove box. On a Schlenk line, carbon dioxide gas (Bone Dry 3.0 Grade Carbon Dioxide, Airgas) was bubbled through the sample, and the clear, colorless liquid became an inhomogeneous slush of clear liquid and white solid (Figure S1). The sample was kept in the septum-capped cuvette and stored in a fume hood, and was handled under atmospheric conditions for all further experiments. The white slush in the mixture melted at $\sim 60\text{-}70^\circ\text{C}$ to form a clear, colorless, homogeneous solution. When the solution was removed from heat, it formed an opaque white solid.

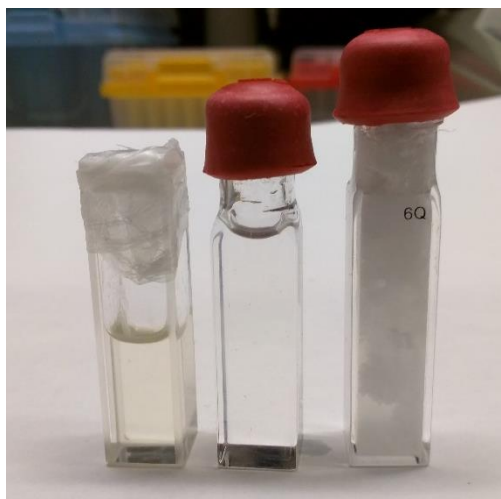


Figure S1. Oleylamine ($\geq 98\%$ primary amine) as-received (left), purified and dried (middle), and purified and dried oleylamine after dry carbon dioxide gas was bubbled through (right).

The samples shown in Figure S1 were investigated with attenuated total reflection infrared (ATR-IR) spectroscopy (Cary 630 FTIR Spectrometer, Agilent) in air, and the spectra are shown in Figure S2. The as-received oleylamine sample and the purified and dried oleylamine sample were liquids during the measurement. In contrast, the purified and dried oleylamine sample that dry carbon dioxide gas had been bubbled through was a slush; a sampling press removed residual liquid for the ATR-IR measurement. The ATR-IR spectrum of the solid formed after CO_2 was bubbled through oleylamine has peaks consistent with literature spectra of other ammonium carbamates,^{11, 13-15} and is presumed to come from an ammonium carbamate. The reversibility of this reaction was not investigated.

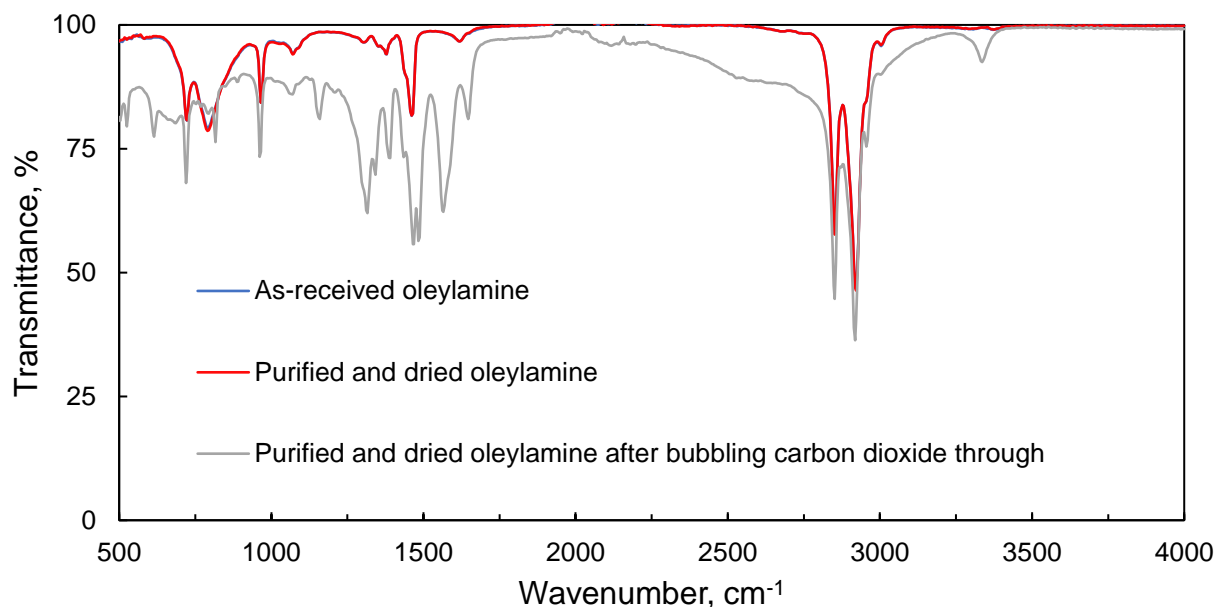
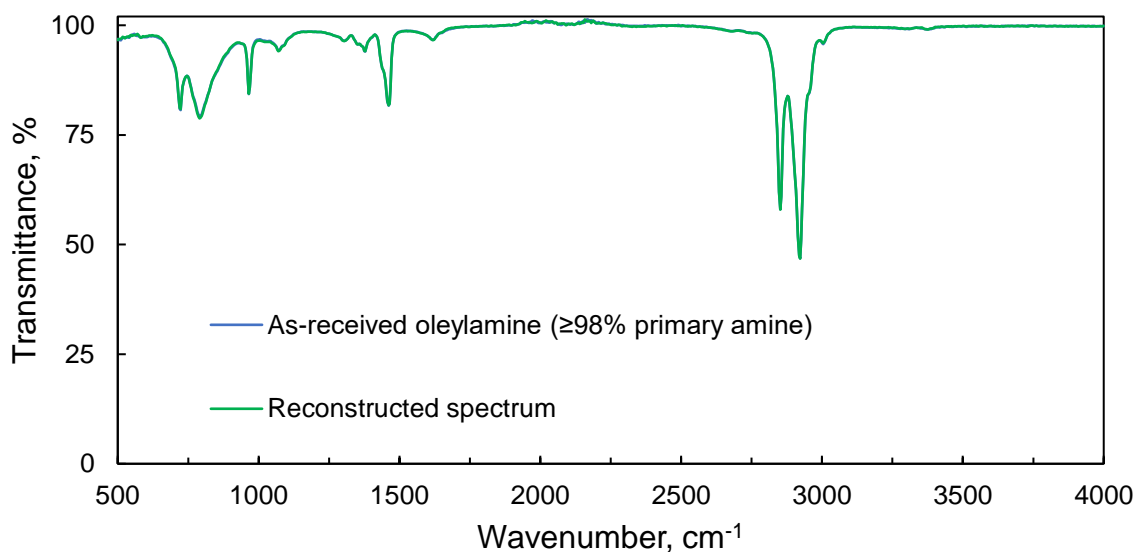


Figure S2. Attenuated total reflection infrared (ATR-IR) spectra of oleylamine ($\geq 98\%$ primary amine) as-received (blue), purified and dried (red), and the solid formed by bubbling dry carbon dioxide gas through purified and dried oleylamine (gray). The two oleylamine samples were liquids, and the oleylamine sample that was exposed to carbon dioxide was pressed into a solid.

An upper bound for ammonium carbamates present in as-received oleylamine ($\geq 98\%$ primary amine) was estimated by reconstructing the ATR-IR spectrum of as-received oleylamine from a weighted sum of the purified and dried oleylamine spectrum and the ammonium carbamate spectrum (baseline subtracted and scaled so that the intensity of the $\sim 966\text{ cm}^{-1}$ peak matched that of the purified and dried oleylamine spectrum). The weights were calculated by linear regression with a constant offset. The calculated weight of the purified and dried oleylamine spectrum is 0.988, the calculated weight of the ammonium carbamate spectrum is 0.005, and the calculated constant offset is 0.682. Dividing the weight of the ammonium

carbamate spectrum by the sum of the weights, the ammonium carbamate impurity in as-received oleylamine can account for no more than 0.5% of the ATR-IR spectrum. Figure S3a shows the spectrum of the as-received oleylamine and its reconstructed spectrum. Figure S3b shows the residual spectrum (spectrum of as-received oleylamine minus the weighted spectrum of purified and dried oleylamine and the constant offset), which has no features resembling the ammonium carbamate spectrum (Figure S2, gray trace). There is no evidence for ammonium carbamates in the as-received oleylamine sample, which had been opened over a year before and stored in a cabinet.

a)



b)

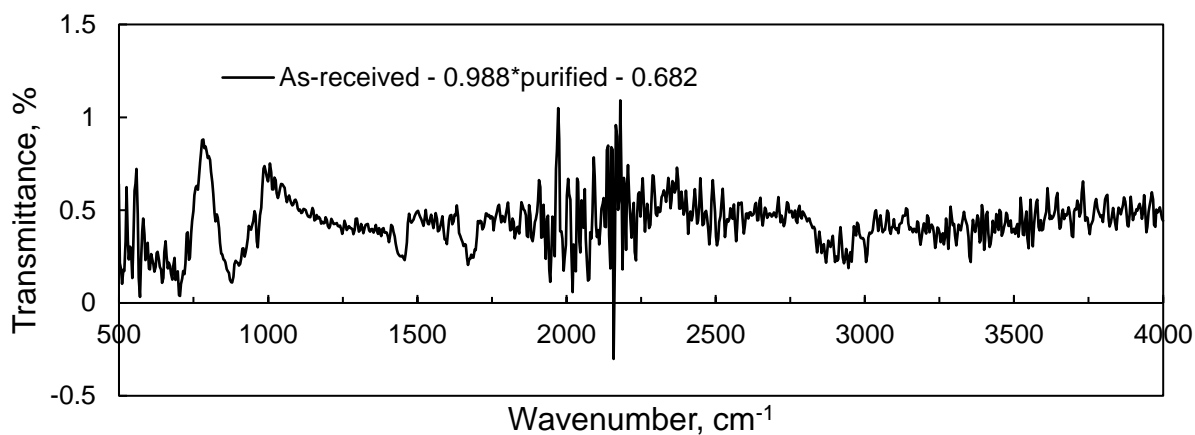


Figure S3. a) Comparison of the ATR-IR spectra of as-received oleylamine ($\geq 98\%$ primary amine) (blue) and its spectrum reconstructed from the weighted sum of the spectra of purified and dried oleylamine and ammonium carbamates from oleylamine (green). b) Residual between the spectrum from as-received oleylamine and the spectrum of the purified and dried oleylamine spectrum with constant offset.

5) Precipitation Tests for Lead Chloride and Sulfur with Acetonitrile Non-Solvent

In the glovebox, 63.6 mg PbCl_2 (99.999%, ultra dry, packaged under Argon, Alfa Aesar, stored in the glovebox and massed outside of the glove box in a vial capped with a PTFE-lined screw cap to maintain an inert atmosphere) was dissolved in 1 mL purified and dried oleylamine (technical grade, 70%, Aldrich, lot #STBD9442V) at $\sim 120^\circ\text{C}$ for 20 minutes while stirring vigorously with a stir bar. The hot plate was turned off, allowing the solution to cool towards the glove box temperature (32°C) for ~ 2 hours (it remained liquid, indicating a liquidus temperature below 32°C at this mole fraction) before 1.1 mL toluene (99.8%, anhydrous, $<0.001\%$ water, Sigma-Aldrich, lot #SHBJ3223) was added. Acetonitrile (extra dry, $<10\text{ppm}$ water, Acros, lot #B00P0305) was added in aliquots of $32\ \mu\text{L}$ (while stirring) until ~ 1.12 mL was added. At that point a persistent precipitate was observed. (Before that point a precipitate would appear upon acetonitrile addition but would redissolve within 5 seconds.) For this lead chloride in oleylamine solution, the PbCl_2 mole fraction was 0.075, and the final acetonitrile proportion was 34.8% v/v relative to the volumes of acetonitrile, oleylamine, and toluene combined. (In a prior test at similar concentration, the liquidus temperature was above the glove box temperature and the white precipitate formed at 34% v/v acetonitrile.)

In the glovebox, 8.3 mg sulfur (99.999%, Strem Chemicals Inc, lot #30456400, stored in the glovebox and massed outside of the glove box in a vial capped with a PTFE-lined screw cap to maintain an inert atmosphere) was dissolved in 1 mL purified and dried oleylamine (technical grade, 70%, Aldrich, lot #STBD9442V) at $\sim 32^\circ\text{C}$ with a stir bar spinning overnight, and then 1.1 mL toluene (99.8%, anhydrous, $<0.001\%$ water, Sigma-Aldrich, lot #SHBJ3223) was added. Acetonitrile (extra dry, $<10\text{ppm}$ water, Acros, lot #B00P0305) was added in aliquots of $32\ \mu\text{L}$ (while stirring) until ~ 1.6 mL was added. No precipitation was observed. For this sulfur in oleylamine solution, the S mole fraction was 0.085, and the final acetonitrile proportion was 43.2% v/v relative to the volumes of acetonitrile, oleylamine, and toluene combined.

6) Lead Sulfide Quantum Dot Synthesis

Following a literature synthesis¹⁶ with the modifications described in the main text, PbS quantum dots were synthesized using purified, dried, and filtered oleylamine (70% technical grade, Aldrich, Lot # STBD9442V). The synthesis described here has three additional differences from that described in ref.¹⁶: the Pb:S ratio is ~9:1, the hot injection temperature is 90° C, and the entire synthesis was performed in a nitrogen-filled glove box.

In a 50 mL round bottom flask with a magnetic stir bar (egg-shaped, 3/4 x 3/8", PTFE coated, Fisher), 0.9053 g of ground lead chloride (anhydrous, 99.999%, Alfa Aesar, Lot # T17A004) was mixed with 7.5 mL of oleylamine. The flask was capped with a PTFE tape-wrapped rubber septum, and the white suspension was stirred on a stir plate at 600 RPM. The suspension was heated with a heating mantle and formed a clear, colorless solution by the time the temperature had reached 120°C. The solution was kept at 120°C for ~30 minutes, and then the temperature was reduced to 90.5°C. In the meantime, a 6 mg/mL solution of sulfur in oleylamine was prepared by dissolving 0.0140 g of ground sulfur (99.999%, Strem, Lot # 30456400) in 2.33 mL of oleylamine upon shaking in a 4 mL glass vial sealed with a PTFE-lined screw cap, forming a clear, orange solution.

Within one hour of preparing the sulfur in oleylamine solution, 2 mL (not the entire 2.33 mL) of the sulfur in oleylamine solution was drawn into a 2 mL glass syringe with a needle attached. The needle was removed, and the solution was kept in the syringe by holding the plunger steady by hand. To reduce splashing, the stirring speed of the lead chloride in oleylamine solution was reduced to 400 RPM, the rubber septum was removed from the round bottom flask, and the glass syringe (without the needle) containing the sulfur in oleylamine solution was lowered into the round bottom flask. The sulfur in oleylamine solution was then injected into the lead chloride in oleylamine solution, and the septum cap was replaced. The

resulting solution was dark brown. Seven minutes after the injection, the reaction was quenched by removing the rubber septum and pouring 12 mL of toluene (99.8%, anhydrous, <0.001% water, Sigma-Aldrich) into the flask via a glass funnel. The flask was removed from heat and submerged in a bath of tetrachloroethylene at 15°C for ~10 minutes.

Then, the solution was divided into three 15 mL plastic centrifuge tubes. The following washing procedure was performed on one of the three vials. The sample was centrifuged at 3000 RPM for 3 minutes, and no precipitate was observed. To precipitate quantum dots from the solution, 2 mL of acetonitrile (extra dry, < 10 ppm water, Acros, Lot # B00P0305) was added. The sample was shaken and centrifuged at 3000 RPM for ~30 seconds, after which a precipitate was observed. The supernatant (clear brownish yellow – allowing the possibility that this precipitation may be somewhat size-selective) was discarded, and the precipitate (dark chocolate brown) was dissolved in 5 mL of toluene (instead of the solution of oleic acid in toluene usually used to exchange ligands at this point^{16, 17}). The quantum dots were precipitated again by adding 1.5 mL of acetonitrile to the solution, shaking, centrifuging for 3 minutes at 3000 RPM, and discarding the supernatant (cloudy gray). The above washing procedure took less than 30 minutes. The precipitate (dark chocolate brown) was dried in the glove box antechamber under vacuum for one hour. The dried quantum dot precipitate (dark chocolate brown) was then dissolved in cyclohexane-d₁₂ (≥99.6 atom % D, Aldrich, Lot # MBBC3402) for measurement of the visible absorbance spectrum (Figure S4) and the ¹H NMR spectrum (Figure S5).

PbS quantum dots synthesized using purified, dried, and filtered oleylamine (≥ 98% primary amine, Aldrich, Lot # MKBZ7016V) were synthesized as described above with the following differences. The Pb:S precursor ratio was ~8:1 (0.860 g PbCl₂), a 3 mL glass syringe was used to inject 2 mL of the sulfur in oleylamine solution into the lead chloride in oleylamine

solution, and the temperature of the tetrachloroethylene bath was $\sim 10^{\circ}\text{C}$. After quenching the reaction and dividing into three centrifuge tubes, the quantum dots from one of the vials were initially precipitated with 1.5 mL of acetonitrile (centrifuged and isolated as described above). The resulting precipitate was washed as described above (dissolved in 5 mL of anhydrous toluene, precipitated with 1.5 mL acetonitrile, centrifuged, and supernatant discarded) twice. The dried precipitate was dissolved in cyclohexane- d_{12} for ^1H NMR (Figure S5).

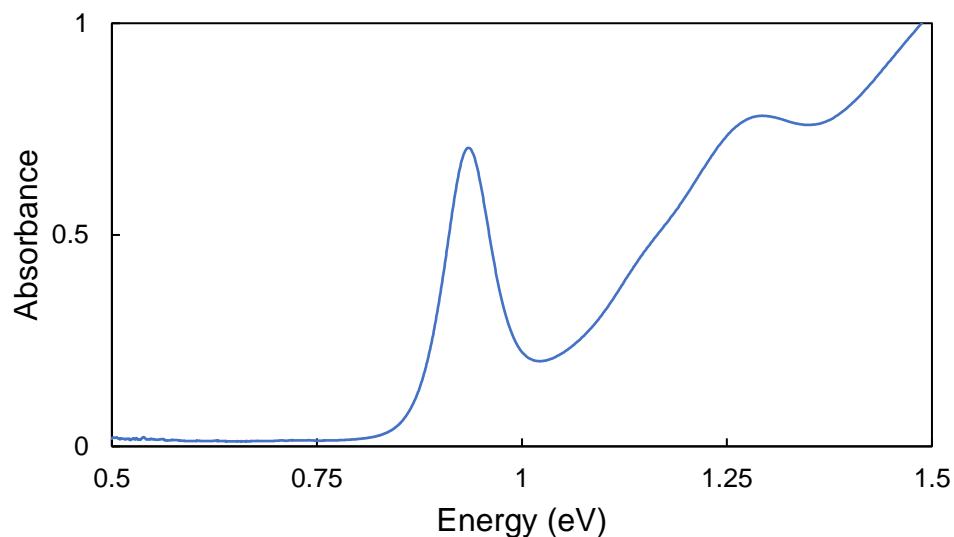


Figure S4. Absorption spectrum of oleylamine capped PbS quantum dots synthesized from sulfur and lead chloride in purified, dried, and filtered oleylamine (70% technical grade), washed, dried, and then dissolved in cyclohexane- d_{12} , as described in SI Section 6. The measurement was taken in a sealed 1 mm quartz cuvette prepared in the glove box. The absorption spectrum of cyclohexane- d_{12} , taken in a similar cuvette, was subtracted from the quantum dot absorption spectrum (baseline offset below 0.75 eV may be a subtraction artifact). The 1S-1S peak has a red-edge HWHM of ~ 35 meV, slightly larger than the HWHM reported for oleate-capped PbS quantum dots with similar bandgap in ref.¹⁶ (32.2 meV for 0.93 eV bandgap).

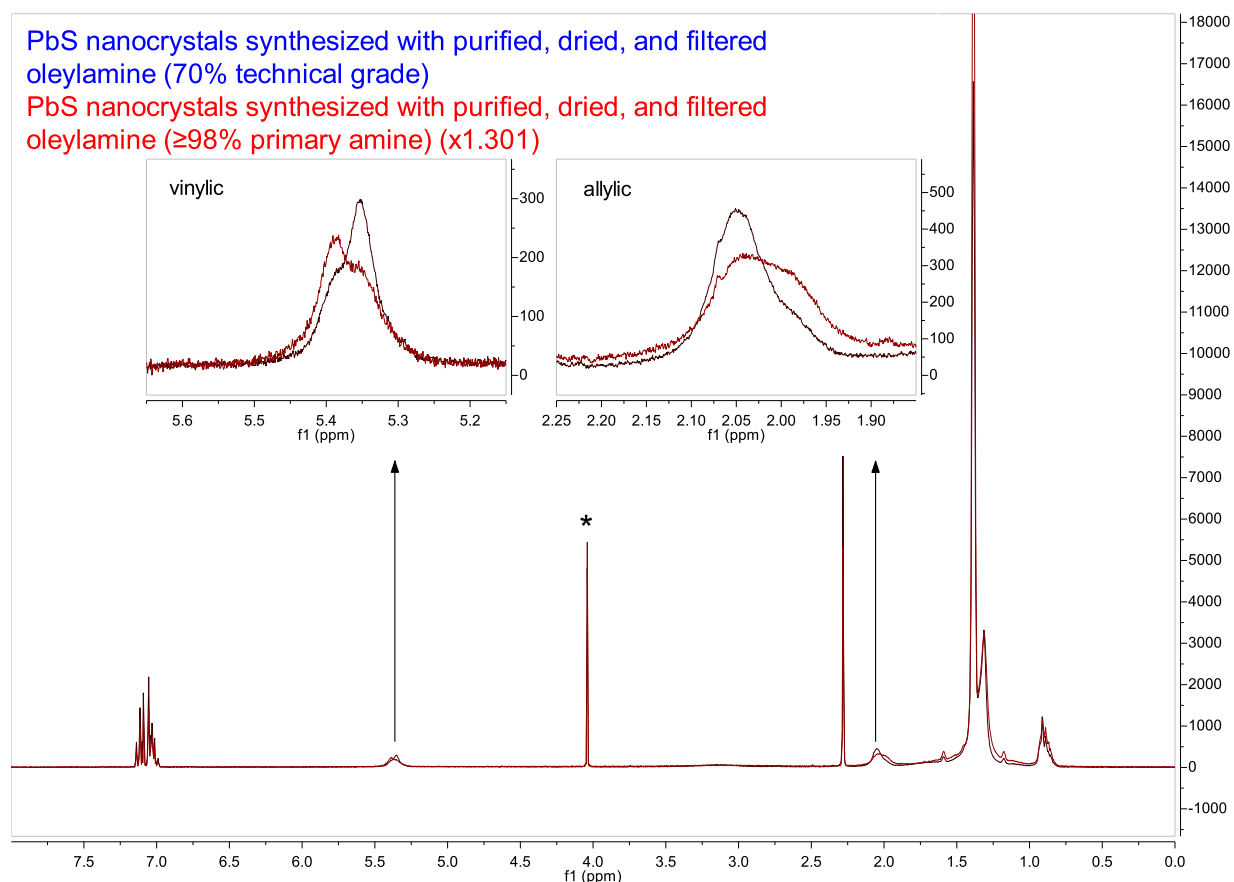


Figure S5. ^1H NMR (300 MHz, cyclohexane- d_{12}) spectra (32 scans, 15 s delay) of PbS nanocrystals synthesized using purified, dried, and filtered oleylamine (70% technical grade) (blue trace), and PbS nanocrystals synthesized using purified, dried, and filtered oleylamine ($\geq 98\%$ primary amine) (red trace), prepared as described in SI Section 6. The spectrum of the PbS nanocrystals synthesized with the “ $\geq 98\%$ primary amine” reagent is scaled to match the area under the vinyl peak of the PbS nanocrystals synthesized with the “70% technical grade” reagent. The chemical shift is referenced to ferrocene (δ^{H} [$\text{Fe}(\text{C}_5\text{H}_5)_2$] = 4.04 ppm in cyclohexane- d_{12} , marked with asterisk) as the internal standard.⁴ Insets show zoomed in portions of the spectra containing signals from vinylic and allylic protons (see Figure 2 in the main text). In the oleylamine reagents, the *trans* vinylic peak is shifted downfield from the *cis* vinylic peak, and the *trans* allylic peak is shifted upfield from the *cis* allylic peak. Relative to the oleylamine reagents in cyclohexane- d_{12} (see Figure 2 in the main text, SI Section 14), the vinylic and allylic resonances are both shifted slightly downfield and broadened for the PbS samples. Shifted and broadened resonances are consistent with bound ligands.¹⁸ The change in lineshape for these resonances between “70% technical grade” and “ $\geq 98\%$ primary amine” proves that both *cis* and *trans* isomers are bound to PbS nanocrystals. Assuming the *cis* vs. *trans* splittings for oleylamine bound to PbS are similar to those in the oleylamine reagents, the lineshapes indicate that more *trans* isomer is bound to PbS nanocrystals synthesized with the “ $\geq 98\%$ primary amine” oleylamine reagent than those synthesized with the “70% technical grade” oleylamine reagent. This roughly parallels the higher ratio of *trans* impurities found in the “ $\geq 98\%$ primary amine” reagent than in the “70% technical grade” reagent.

7) Tables of proton integrals

Table S1. Proton integrals in the ^1H NMR spectra of high purity oleic and elaidic acids in C_6D_{12} , C_6D_6 , and CD_2Cl_2 solvents. In C_6D_6 , signals from methylene protons in the chain ($N_{\text{H}} = 20$) are overlapped with the signal from β -methylene protons ($N_{\text{H}} = 2$), and signals from allylic protons ($N_{\text{H}} = 4$) are overlapped with signals from α -methylene protons ($N_{\text{H}} = 2$), so overall integrals are reported in the respective entries of the table, marked with a “*” and “***”, respectively. All integrals are normalized to the area under the methyl group signal, which is normalized to 3 (the number of protons in CH_3). Corresponding ^1H NMR spectra are shown in Section 14 (pages S36-S41), in the same order as the entries in the table.

d-solvent, compound	CH_3	10 x CH_2	2 x CH_2 , allylic	2 x CH , vinylic	β - CH_2	α - CH_2	COOH
Calculated	3	20	4	2	2	2	1
<i>C₆D₁₂</i>							
Oleic acid	3	solvent interference	4.09	2.02	2.07	2.06	0.98
Elaidic acid	3	solvent interference	4.00	1.97	2.04	2.00	0.97
<i>C₆D₆</i>							
Oleic acid	3	22.08*	6.04***	1.99	22.08*	6.04***	0.96
Elaidic acid	3	21.93*	5.97***	1.99	21.93*	5.97***	0.87
<i>CD₂Cl₂</i>							
Oleic acid	3	20.42	4.10	1.96	2.10	2.06	0.81
Elaidic acid	3	20.15	4.00	1.94	2.02	1.99	0.70

Table S2. Proton integrals in the ^1H NMR spectra of various amine samples in C_6D_{12} , C_6D_6 , and CD_2Cl_2 solvents. On average, these integrals are accurate to within $\sim 3.5\%$. Corresponding ^1H NMR spectra are shown in Section 14 (pages S42-S51), in the same order as the entries in the table.

Amine sample, d-solvent	CH_3	11 x CH_2 + β - CH_2	2 x CH_2 , allylic	2 x CH , vinylic	α - CH_2	NH_2
Calculated for $\text{C}_{18}\text{H}_{35}\text{NH}_2$	3	24	4	2	2	2
70% (lot #STBD9442V), C_6D_6	3	22.91	3.24	1.71	1.84	1.92
70% purified, CD_2Cl_2	3	24.88	3.42	1.67	2.04	2.03
70% purified, C_6D_{12}	3	n/a	3.34	1.70	1.96	1.88
min. 95%, CD_2Cl_2	3	23.71	3.28	1.69	1.85	1.94
min. 95% purified, C_6D_{12}	3	n/a	3.40	1.81	1.92	2.01
$\geq 98\%$, C_6D_6	3	23.77	3.33	1.75	1.93	1.96
$\geq 98\%$, CD_2Cl_2	3	23.98	3.39	1.73	1.97	1.98
$\geq 98\%$ purified, C_6D_{12}	3	n/a	3.51	1.79	1.98	1.92
$\geq 98\%$ purified, CD_2Cl_2	3	24.11	3.36	1.73	1.94	2.00
$\geq 98\%$ purified, C_6D_6	3	24.21	3.56	1.86	1.96	1.99

Table S3. Various ratios (error bars in parenthesis) between the proton integrals from the prior table as compared to the ratios calculated for pure oleylamine. Error bars for the ratios were calculated by using uncertainty propagation formulas for addition and division plus an assumption that each integral from the preceding table (Table S2) has an independent error of $\pm 3.5\%$.

Amine sample, d-solvent	$\frac{[\text{CH}_2]_{\text{Tot}}}{[\text{NH}_2]}$	$\frac{[\alpha\text{-CH}_2]}{[\text{NH}_2]}$	$\frac{[\text{vinyl}]}{[\text{NH}_2]}$	$\frac{[\text{CH}_3]}{[\text{NH}_2]}$
Calculated for $\text{C}_{17}\text{H}_{35}\text{NH}_2$	15	1	1	1.5
70% (lot #STBD9442V), C_6D_6	14.58 (0.66)	0.96 (0.05)	0.89 (0.04)	1.56 (0.08)
70% purified, CD_2Cl_2	14.95 (0.68)	1.00 (0.05)	0.82 (0.04)	1.48 (0.07)
70% purified, C_6D_{12}	n/a	1.04 (0.05)	0.90 (0.04)	1.60 (0.08)
min. 95%, CD_2Cl_2	14.87 (0.68)	0.95 (0.05)	0.87 (0.04)	1.55 (0.08)
min. 95% purified, C_6D_{12}	n/a	0.96 (0.05)	0.90 (0.04)	1.49 (0.07)
$\geq 98\%$, C_6D_6	14.81 (0.67)	0.98 (0.05)	0.89 (0.04)	1.53 (0.08)
$\geq 98\%$, CD_2Cl_2	14.82 (0.67)	0.99 (0.05)	0.87 (0.04)	1.52 (0.08)
$\geq 98\%$ purified, C_6D_{12}	n/a	1.03 (0.05)	0.93 (0.05)	1.56 (0.08)
$\geq 98\%$ purified, CD_2Cl_2	14.71 (0.67)	0.98 (0.05)	0.87 (0.04)	1.50 (0.07)
$\geq 98\%$ purified, C_6D_6	14.94 (0.68)	0.98 (0.05)	0.93 (0.05)	1.51 (0.07)

8) Mass spectra

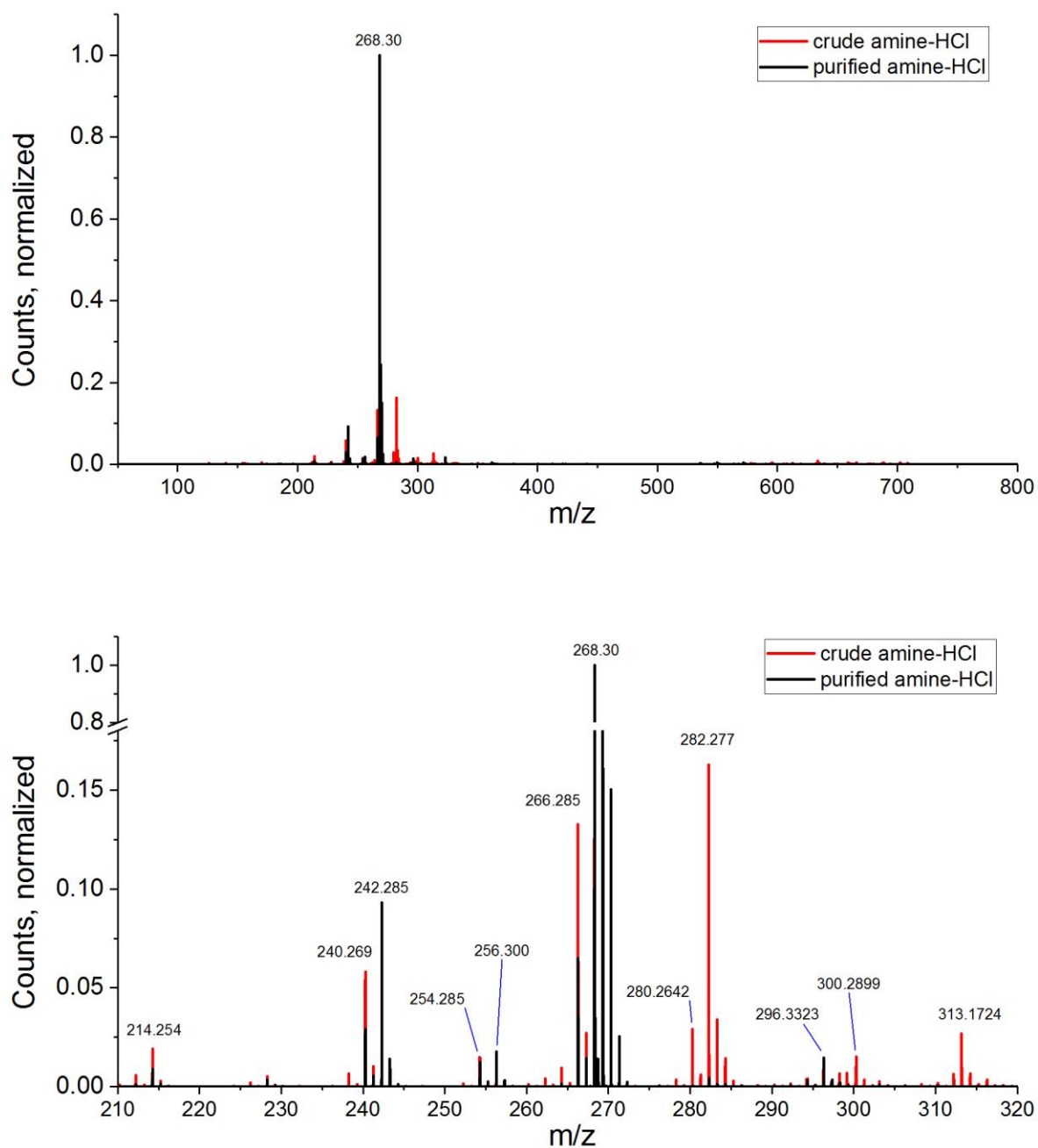


Figure S6. High-resolution mass spectra of crude and purified amine hydrochloride derived from $\geq 98\%$ primary amine sample.

9) Table of mass spectra peaks

Table S4. Observed m/z values for most abundant peaks (^{12}C , ^1H , ^{14}N) with molecular formulas matched to within 0.003 m/z difference. For this rough comparison between crude and purified 98% primary amine, counts for the primary isotope of each species were normalized to the height of the primary isotope of the parent ion (m/z = 268.3006) and reported without correction for each compound's natural isotopic distribution.

m/z, z = 1	empirical formula	exact mass, amu	difference, amu	formula change from the parent ion	counts, norm. <i>crude</i>	counts, norm. <i>purified</i>
214.25376	C ₁₄ H ₃₂ N	214.25347	0.00029	-4xCH ₂ ,+2H	0.02	0.01
240.26947	C ₁₆ H ₃₄ N	240.26912	0.00035	-2CH ₂	0.06	0.03
242.28488	C ₁₆ H ₃₆ N	242.28477	0.00011	-2xCH ₂ ,+2H	0.05	0.09
254.24846	C ₁₆ H ₃₂ NO	254.24839	0.00007	-2CH ₂ , -2H, +O	0.01	0
254.28523	C ₁₇ H ₃₆ N	254.28477	0.00046	-CH ₂	0.01	0.01
256.30033	C ₁₇ H ₃₈ N	256.30042	9E-05	-CH ₂ , +2H	0.01	0.02
266.28497	C ₁₈ H ₃₆ N	266.28477	0.0002	-2H	0.13	0.07
268.3006	C₁₈H₃₈N	268.30042	0.00018	parent	1	1
280.26415	C ₁₈ H ₃₄ NO	280.26404	0.00011	-4H, +O	0.03	<0.001
282.27698	C ₁₈ H ₃₆ NO	282.27969	0.00271	-2H, +O	0.16	<0.001
282.32048 [#]	C ₁₉ H ₄₀ N	282.31607	0.00441	+CH ₂	<0.01	<0.01
296.25849	C ₁₈ H ₃₄ NO ₂	296.25896	0.00047	-4H, +2O	~0.01	<0.001
296.33158	C ₂₀ H ₄₂ N	296.33172	0.00014	+2CH ₂	~0.01	~0.02
300.28996	C ₁₈ H ₃₈ NO ₂	300.29026	0.0003	+2O	0.02	<0.001
313.17235 [*]	C ₁₉ H ₂₃ NO ₃	313.16779	0.00456	+3O,+C, -15H	0.03	<0.001

[#] - accurate determination of the m/z value is affected by a very intense peak nearby (~0.044 amu away); ^{*} - no better match had been found using only C, H, N, and O elements in the empirical formula;

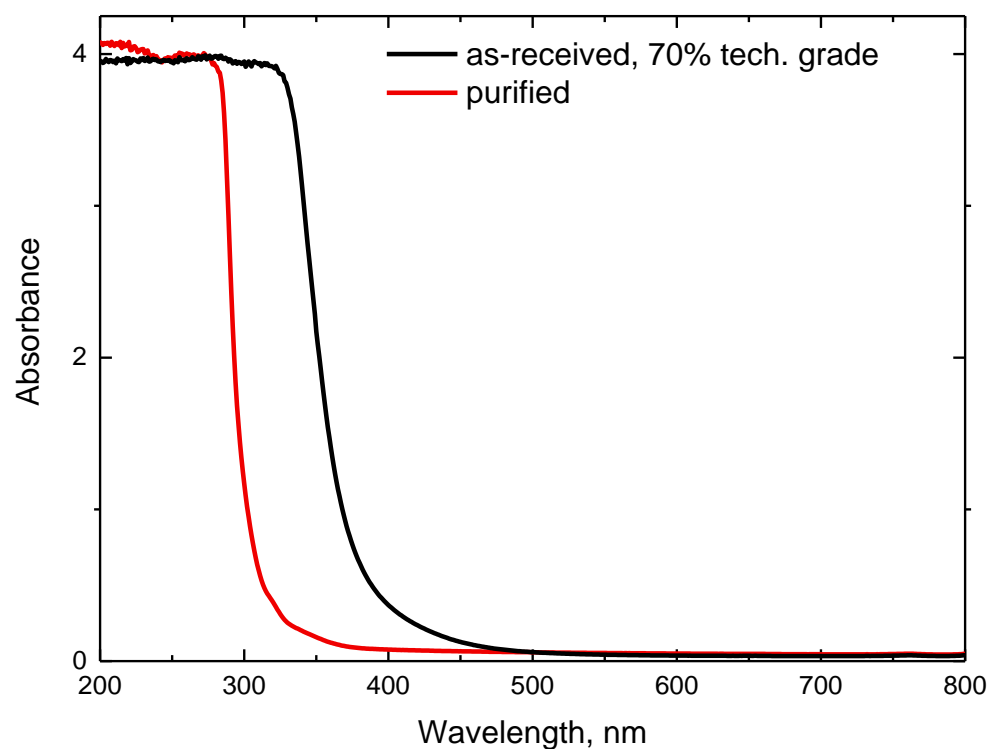
10) UV-Vis absorbance spectra before and after purification

Figure S7. UV-Vis spectra of as-received and purified oleylamine samples of 70% tech. grade reagent recorded in 1 cm pathlength cell. Visually, the as-received sample is a transparent yellow liquid, while the purified sample is a transparent colorless liquid.

11) Table of elemental analyses

Table S5. Results of C, H, and N, elemental analysis (in relative weight percent, wt.%) of three different samples of commercial amine before and after purification. Samples marked with a * were handled under an inert atmosphere for the analysis. “purified” stands for multi-step purification with vacuum distillation over sodium, “dist. only, no Na” stands for purification by only a vacuum-distillation without sodium, “repeat” stands for the replication of the C, H, N, analysis on the same exact sample performed a week later.

Amine	C, wt.%	H, wt.%	N, wt.%	Date of analysis
C₁₈H₃₇N, calculated	80.82	13.94	5.24	-
70% (lot # STBF9554V)	80.90	13.68	5.53	06/09/2017
70% (lot # STBF9554V) purified*	81.19	13.81	5.57	06/09/2017
70% (lot # STBD9442V)	80.80	13.74	5.44	11/09/2016
70% (lot # STBD9442V) repeat	80.78	13.63	5.39	11/16/2016
min. 95% (lot # 21991600)*	80.46	13.99	5.41	06/09/2017
min. 95% (lot # 21991600) purified*	80.85	14.13	5.50	06/09/2017
≥98% (lot # MKBZ7016V)	80.82	14.18	5.55	06/09/2017
≥98% (lot # MKBZ7016V) purified*	80.67	14.02	5.48	06/09/2017
≥98% (lot # MKBZ7016V)	81.08	13.40	5.49	11/09/2016
≥98% (lot # MKBZ7016V) repeat	80.80	14.02	5.56	11/16/2016
≥98% (lot # MKBZ7016V) dist. only, no Na	80.85	13.45	5.67	11/09/2016
≥98% (lot # MKBZ7016V) dist. only, no Na, repeat	80.82	13.83	5.62	11/16/2016
≥98% (lot # MKBZ7016V) purified	81.16	13.10	5.72	11/09/2016
≥98% (lot # MKBZ7016V) purified, repeat	80.89	13.81	5.65	11/16/2016

12) Ratio method as applied to ^1H NMR, Raman, and FTIR spectra

12.1) ^1H NMR

Following the idea of the ratio method for separation of spectra of mixtures,¹⁹⁻²¹ we assumed that a ^1H NMR spectrum of each oleylamine reagent [$S_{reagent}(\delta)$] is a linear sum of weighted spectra of just two components, *cis* and *trans* isomers:

$$S_{reagent}(\delta) = A \cdot cis(\delta) + B \cdot trans(\delta),$$

where A and B are amplitude weights of each isomer, δ is a chemical shift. The weights were determined in three steps. First, a spectral feature belonging to the *cis* component was chosen and reagent spectra were normalized to its intensity. Second, the spectrum of the *trans* component was obtained through the difference between these normalized spectra. The second step was repeated to obtain a spectrum of the *cis* component (through normalization to a spectral feature of the *trans* component). Third, the amplitude weights were found by using a linear least squares fit to minimize the rms difference between each reagent spectrum and the weighted sum of the individual *cis* and *trans* spectra. Once the amplitude weights were determined, relative areas under the peaks (a and b , for *cis* and *trans*, respectively) were calculated, corresponding to the ratio of molar fractions (Table S6). All operations were performed in Microsoft Excel 2016 and MATLAB R2014a.

The three steps are illustrated below for the allylic region in ^1H NMR spectra (2.15-1.85 ppm chemical shift in cyclohexane- d_{12}) of purified 70% technical grade and $\geq 98\%$ primary amine oleylamine reagents.

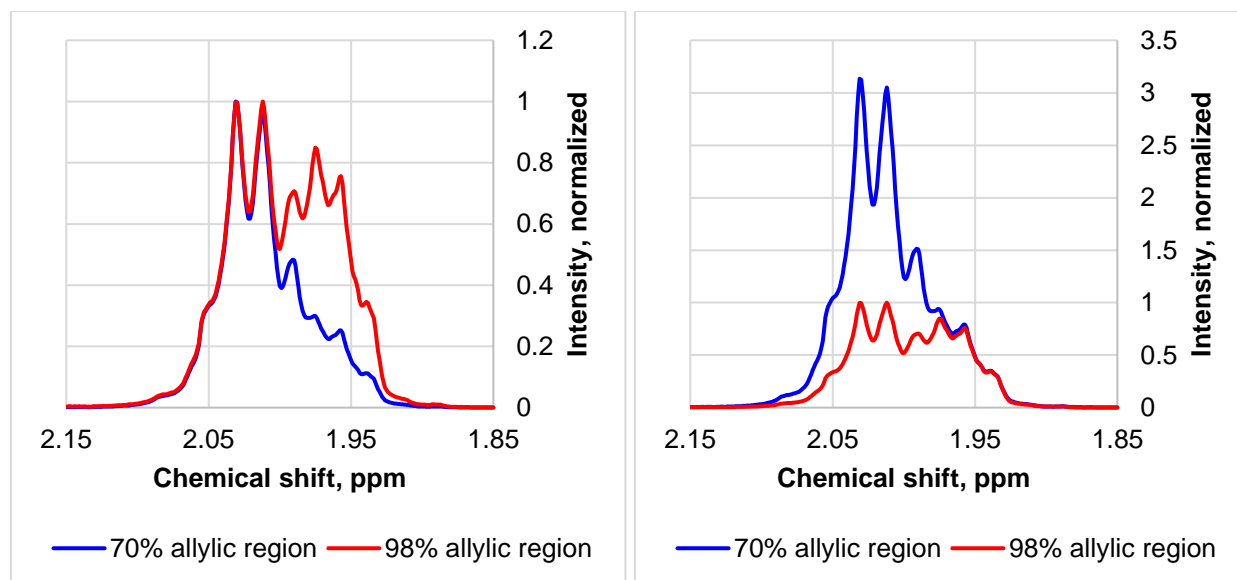


Figure S8. Step 1, allylic region from ^1H NMR spectra of purified 70% technical grade and $\geq 98\%$ primary amine oleylamine reagents normalized to the height of the 2.03 ppm peak (left panel, multiplet of the *cis* isomer) and the 1.93 ppm peak (right panel, multiplet of the *trans* isomer).

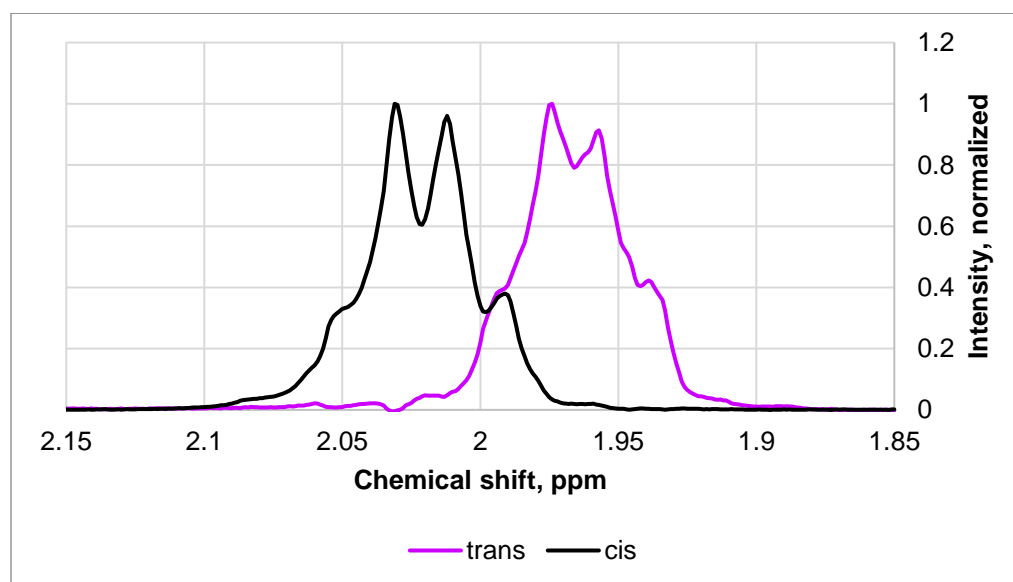


Figure S9. Step 2, allylic NMR spectra of the *cis* (left) and *trans* (right) components obtained from the difference between spectra shown in the preceding figure.

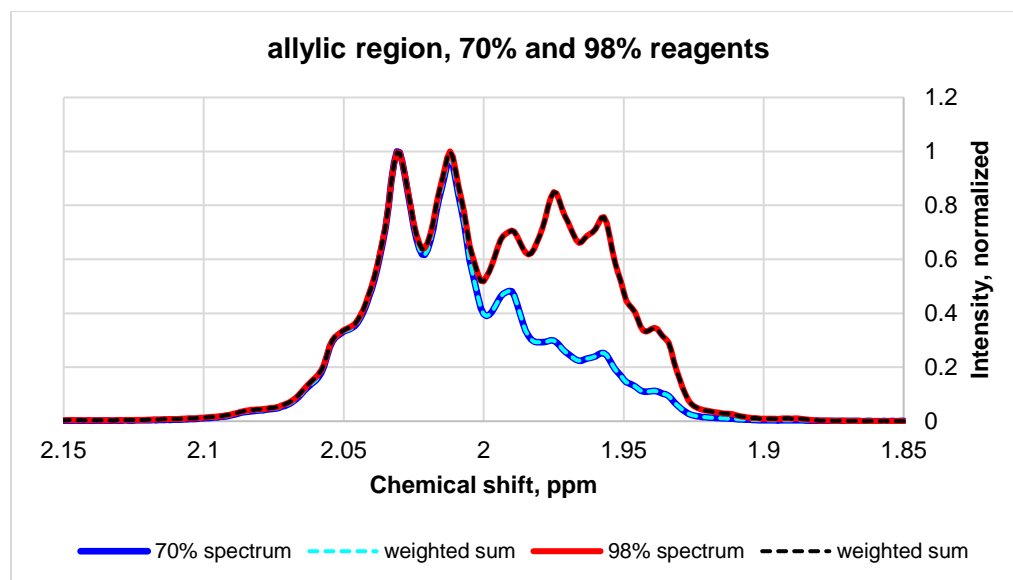


Figure S10. Step 3, allylic region of ^1H NMR spectra fit with a weighted sum of *cis* and *trans* components for 70% ($A = 1, B = 0.259$) and 98% ($A = 1, B = 0.811$) reagents.

Table S6. Summary of the amplitude weights A and B (relative areas, a and b , in parenthesis) obtained for *cis* and *trans* components through ratio method decomposition of allylic and vinylic regions in ^1H NMR spectra of two purified oleylamine reagents.

Reagent, components	^1H NMR	
	Allylic	Vinylic
purified 70% technical grade		
<i>cis</i>	1 (0.786)	1 (0.794)
<i>trans</i>	0.259 (0.214)	0.258 (0.205)
purified $\geq 98\%$ primary amine		
<i>cis</i>	1 (0.524)	1 (0.561)
<i>trans</i>	0.811 (0.476)	0.781 (0.439)

12.2) Raman

The ratio method separation of Raman spectra was performed in three steps. First, Raman spectra of purified 70% technical grade and $\geq 98\%$ primary amine oleylamine reagents were normalized to the height of the $1400\text{--}1500\text{ cm}^{-1}$ band (asymmetric bend of $-\text{CH}_3$ group and scissoring vibrations of $-\text{CH}_2-$ groups) at its height ($\sim 1440\text{ cm}^{-1}$), as it is a peak common to both spectra and should be independent of the content of *cis* and *trans* components. Second, Raman

spectra of individual *cis* and *trans* components were obtained by a difference between spectra of purified 70% technical grade reagent (*cis* rich) and purified $\geq 98\%$ primary amine reagent (*trans* rich) in a way similar to the NMR described above, and individually normalized to the height of the 1400-1500 cm^{-1} band prior to the next step. Third, the amplitude weights for each component were found by using a linear least squares fit to minimize the rms difference between each reagent spectrum and the weighted sum of the individual *cis* and *trans* spectra. All operations were performed in Microsoft Excel 2016 and MATLAB R2014a. Table S7 summarizes the result. In the case of Raman spectra normalized to the 1400-1500 cm^{-1} band, the ratio of each component's amplitude weight to the sum of amplitude weights is the molar fraction of that components.

Table S7. Summary of weights obtained for *cis* and *trans* components for the Raman spectra of two oleylamine reagents.

Reagent, components	Raman
purified 70% technical grade	
<i>cis</i>	0.788
<i>trans</i>	0.212
purified $\geq 98\%$ primary amine	
<i>cis</i>	0.530
<i>trans</i>	0.470

12.3) FTIR

The lack of a strong and well-defined feature for a *cis* component in the FTIR spectra of oleylamine reagents plus over-depletion of the IR beam in the region of the strongest molecular vibrations [symmetric and asymmetric stretches of $-(\text{CH}_2)_n-$] complicated application of the ratio method across the entire spectral range (400-4000 cm^{-1}). Given the close agreement of *cis* to *trans* molar fractions from both ^1H NMR and Raman, their respective averages were used as proportionality coefficients to isolate FTIR spectra of *cis* and *trans* components through the

difference between experimental FTIR spectra of purified 70% technical grade and $\geq 98\%$ primary amine oleylamine reagents (referred to as “70% reagent” and “98% reagent” below for brevity) normalized to the height of the common and *cis/trans* independent spectral feature at $1400\text{-}1500\text{ cm}^{-1}$. The following molar fractions were used:

$$70\% \text{ reagent, } x_{cis}^{70\%} \approx 0.79, x_{trans}^{70\%} \approx 0.21;$$

$$98\% \text{ reagent, } x_{cis}^{98\%} \approx 0.54, x_{trans}^{98\%} \approx 0.46.$$

Thus, the isolated spectrum of the *cis* isomer (Figure S12) was obtained via:

$$cis(\nu) = [x_{trans}^{98\%} \cdot \text{FTIR}_{70\% \text{ reagent}}(\nu) - x_{trans}^{70\%} \cdot \text{FTIR}_{98\% \text{ reagent}}(\nu)].$$

Similarly, the isolated spectrum of the *trans* isomer (Figure S13) was obtained via:

$$trans(\nu) = [x_{cis}^{70\%} \cdot \text{FTIR}_{98\% \text{ reagent}}(\nu) - x_{cis}^{98\%} \cdot \text{FTIR}_{70\% \text{ reagent}}(\nu)].$$

Comparison to the spectra of oleic acid and elaidic acid in Figure S11 shows the isolated FTIR spectra are inaccurate for the strongest C-H stretch bands shaded in gray.

13) FTIR spectra

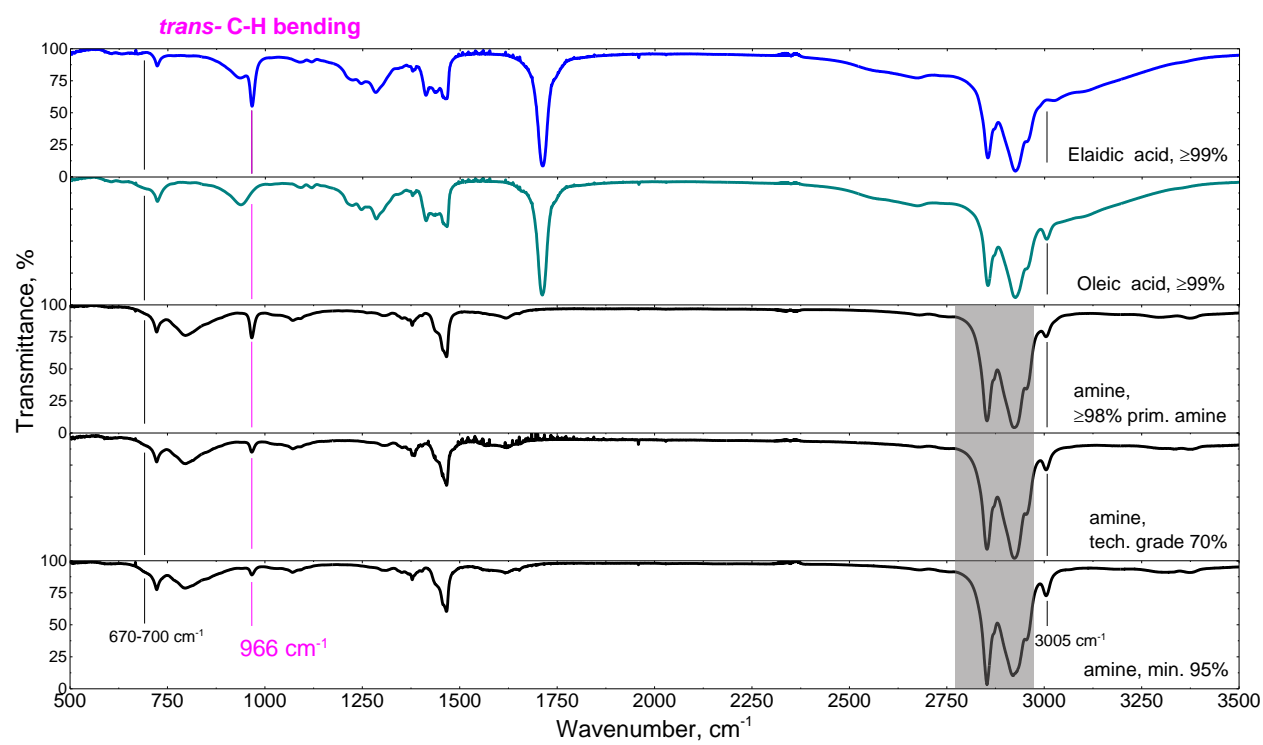


Figure S11. Overlaid experimental FTIR spectra for high purity elaidic and oleic acids, and three purified commercial oleylamine reagents. The strongest C-H stretch bands [symmetric and antisymmetric stretches of $-(CH_2)_n-$] are gray shaded because their lineshapes and relative intensities are distorted by over-depletion of the IR beam.

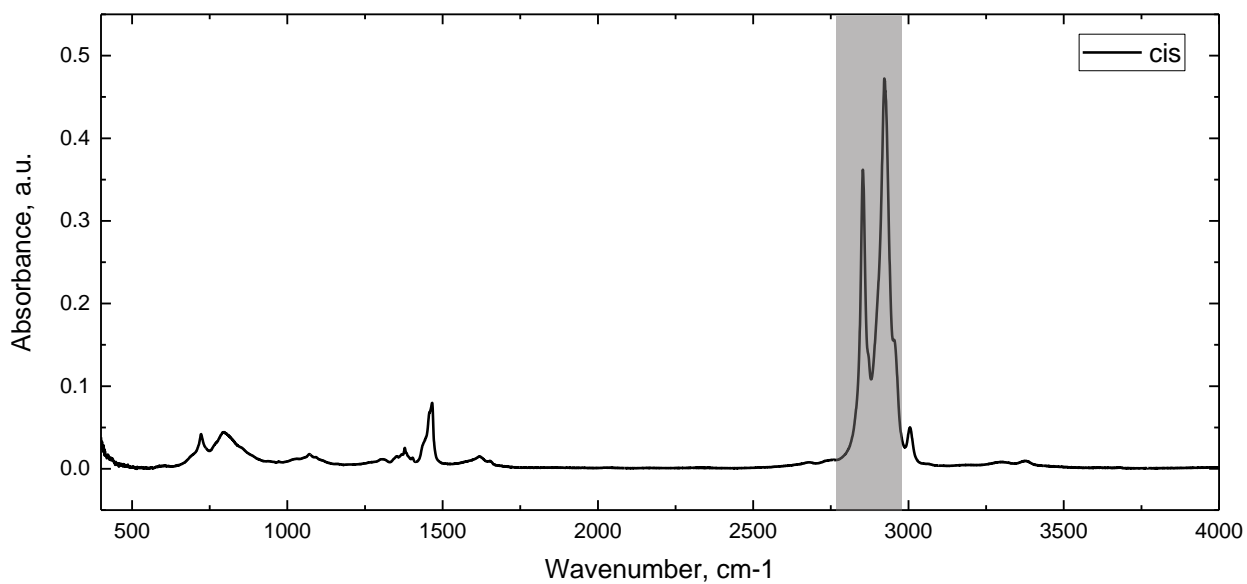


Figure S12. Isolated FTIR spectrum of the *cis* isomer. The strongest C-H stretches [symmetric and antisymmetric stretches of $-(\text{CH}_2)_n-$] are gray shaded as their lineshapes and relative intensities are distorted by over-depletion of the IR beam.

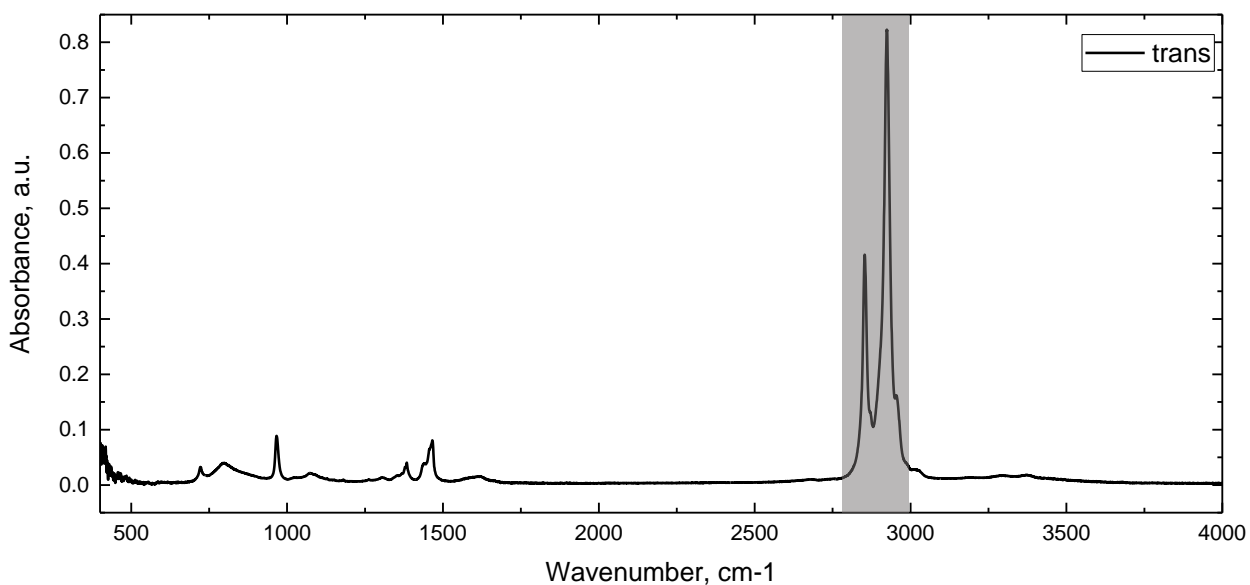
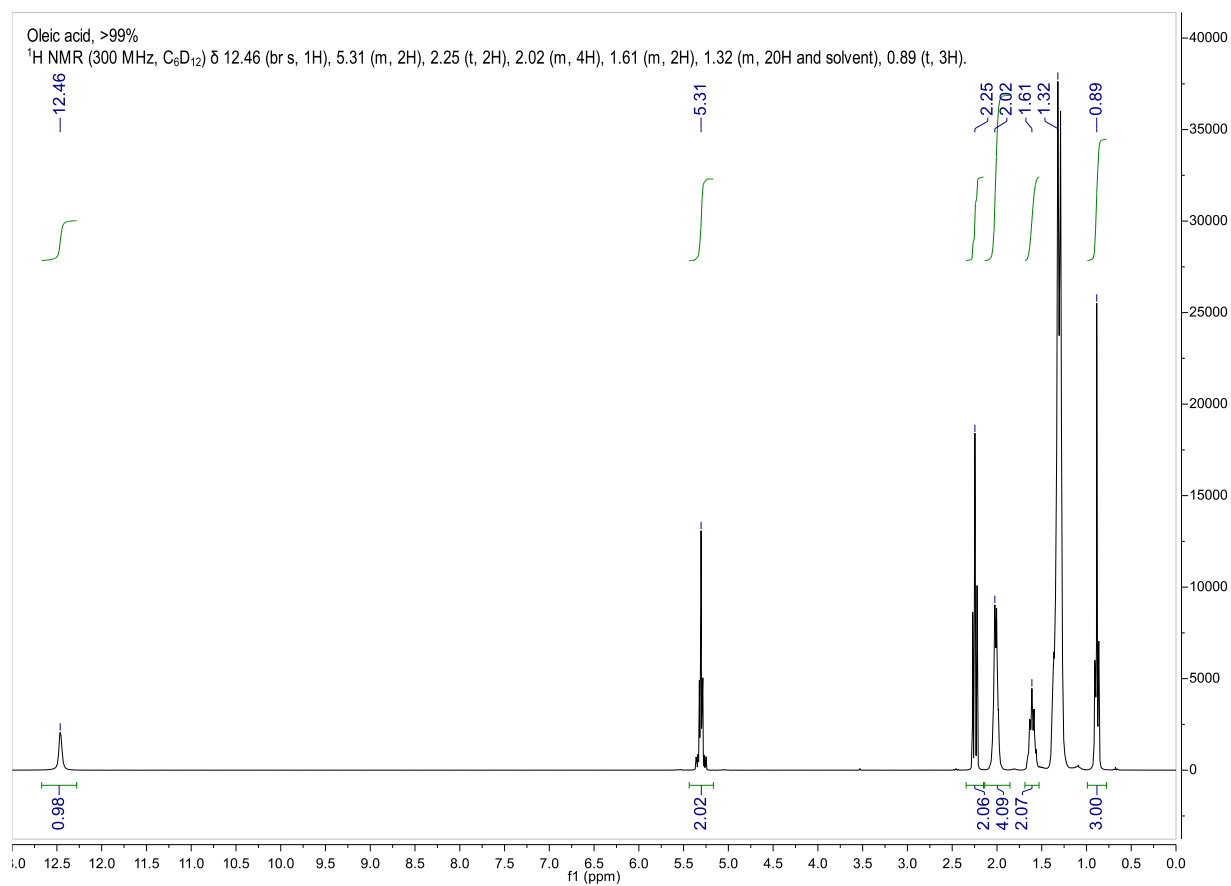
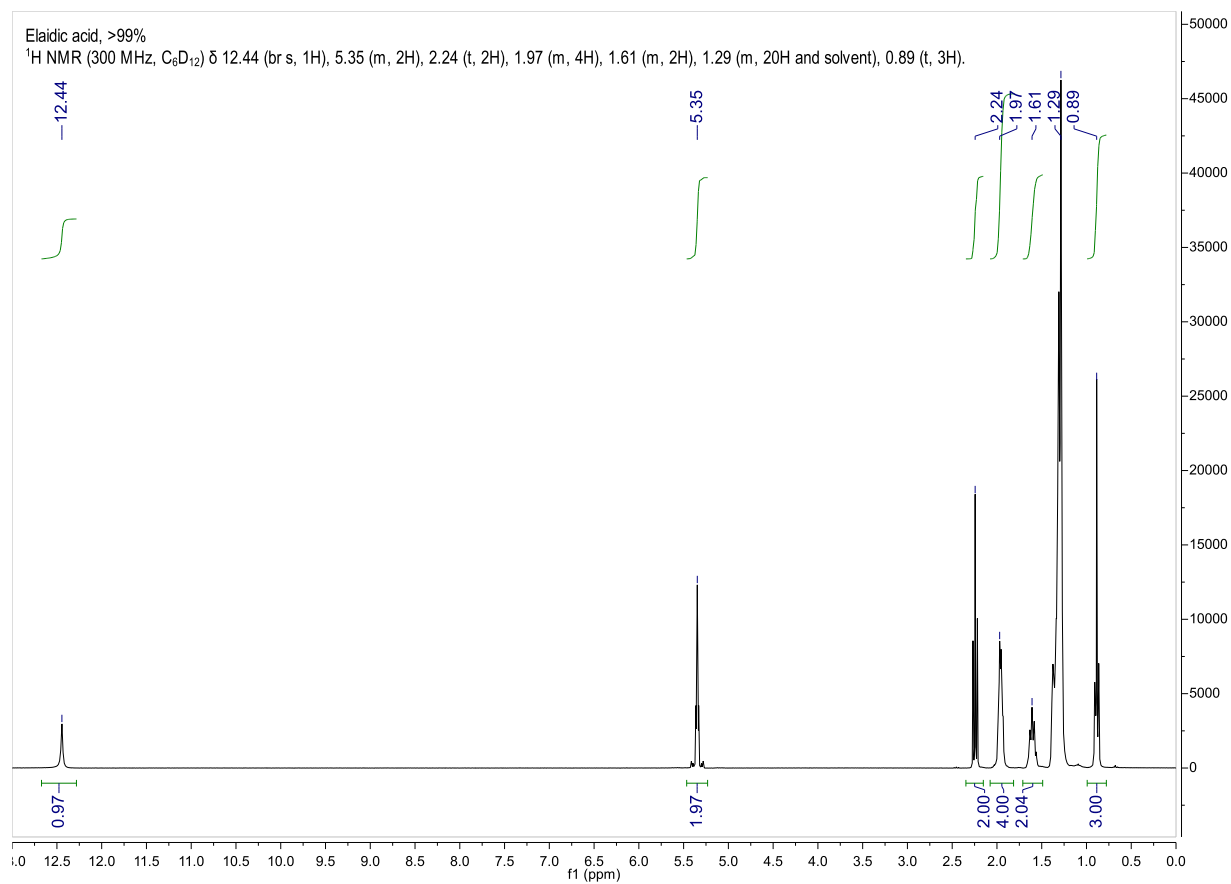
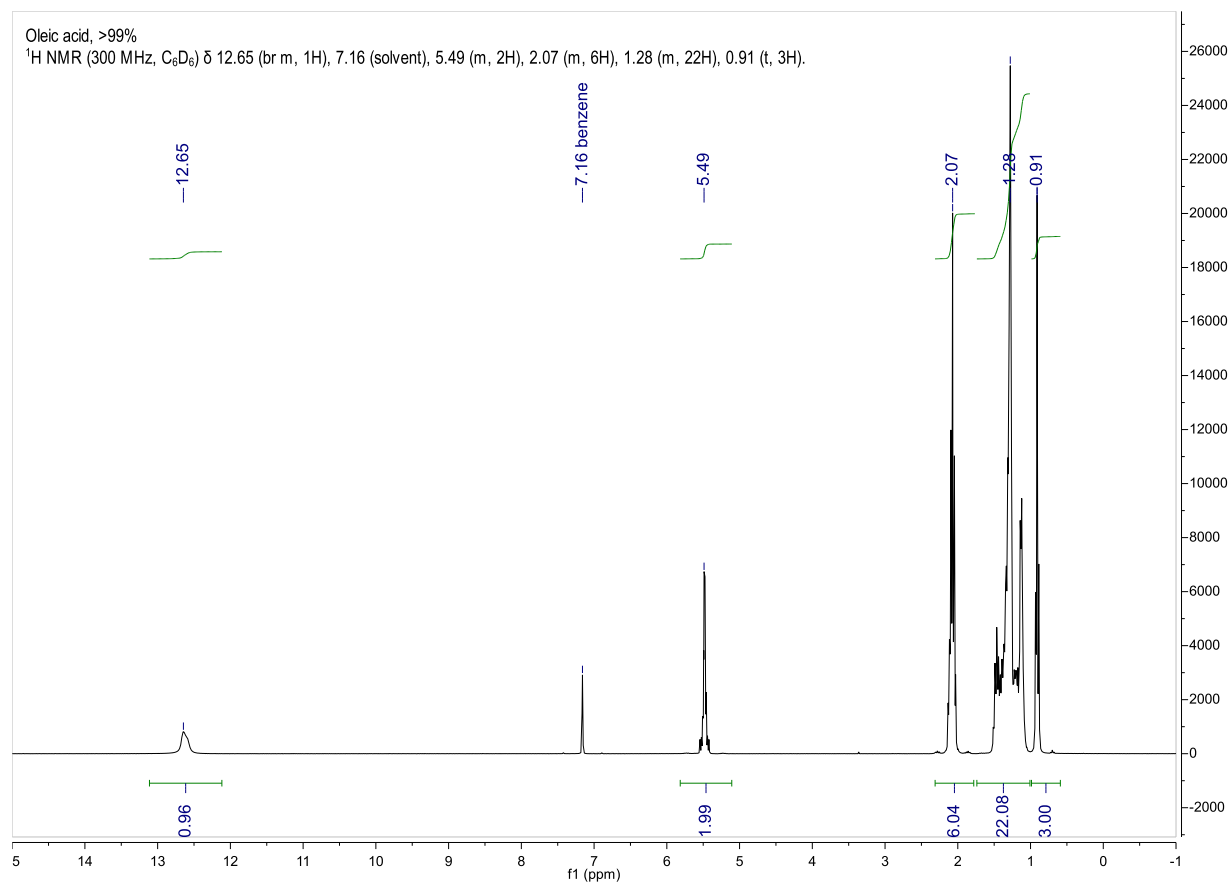
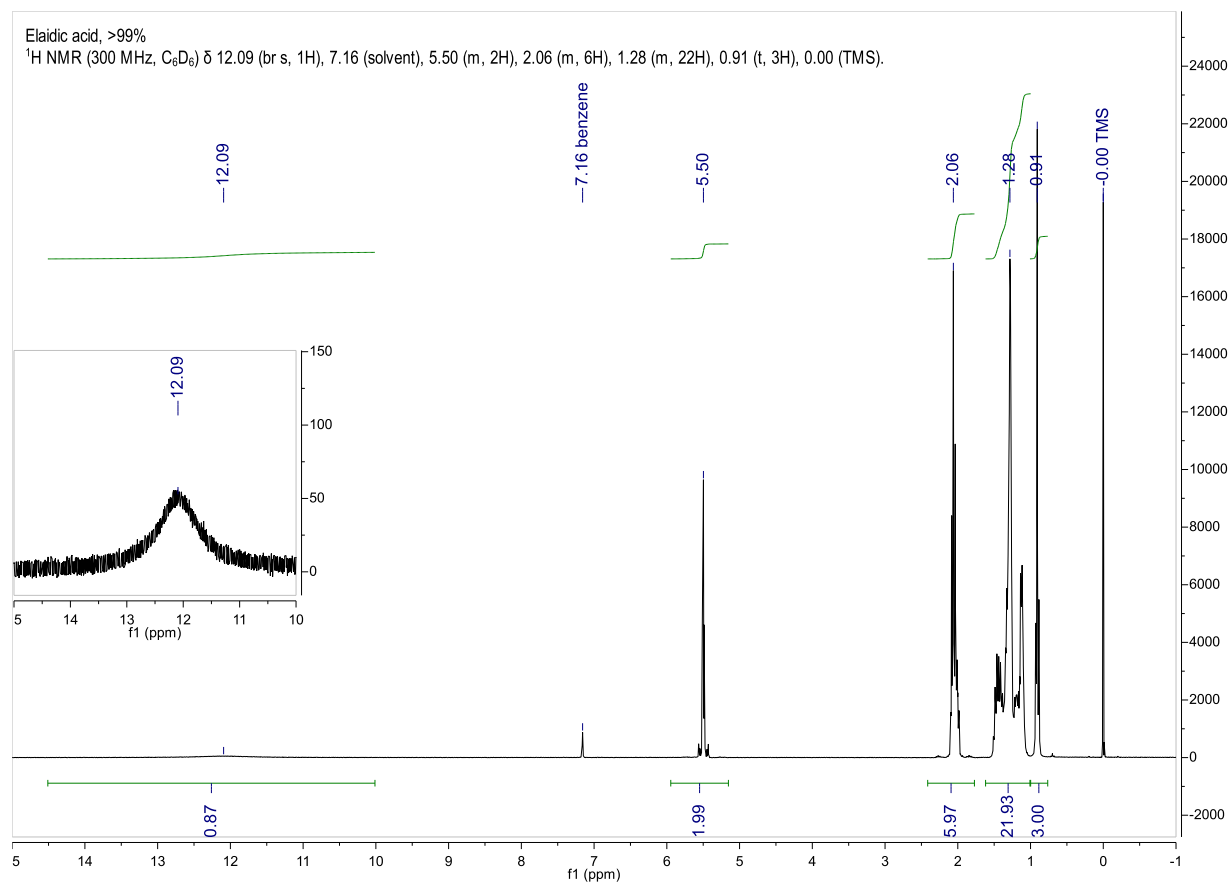


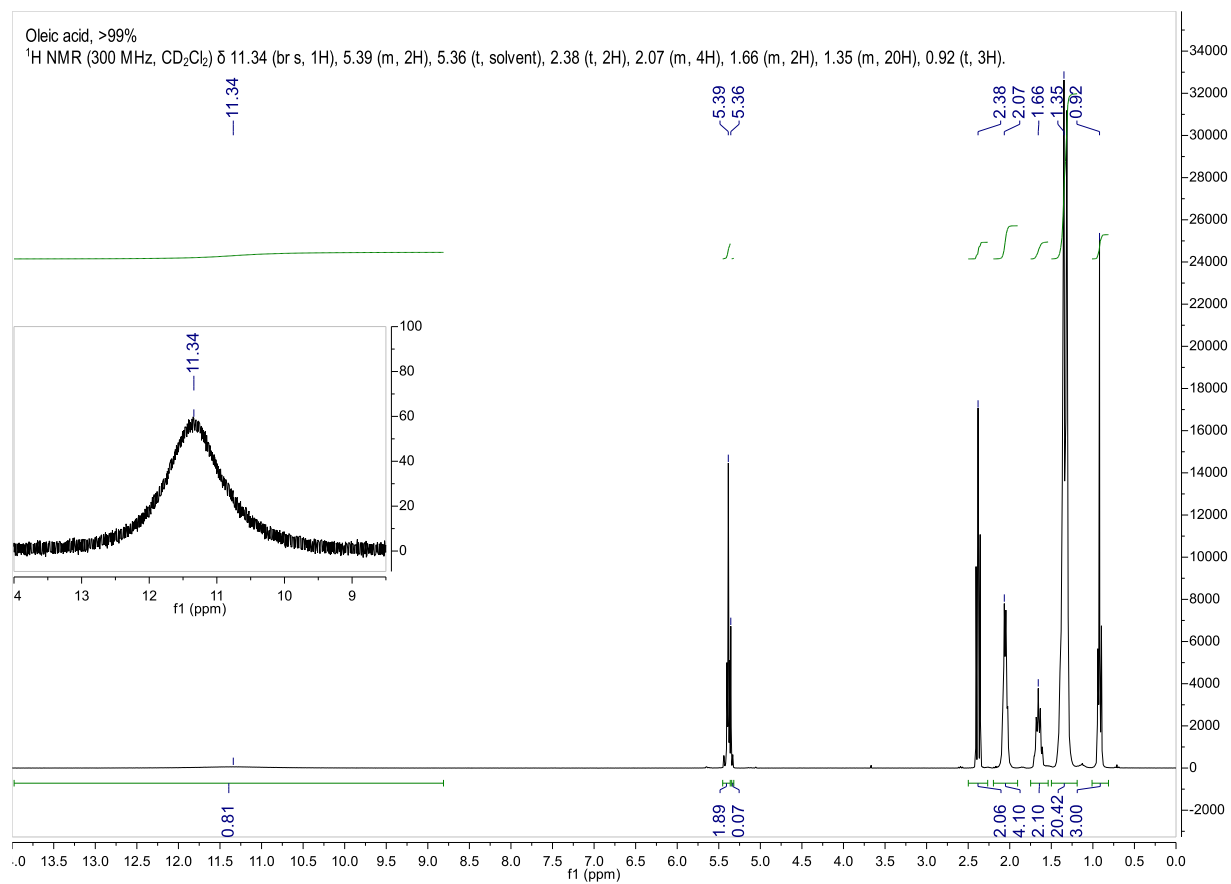
Figure S13. Isolated FTIR spectrum of the *trans* isomer. The strongest C-H stretches [symmetric and antisymmetric stretches of $-(\text{CH}_2)_n-$] are gray shaded because their lineshapes and relative intensities are distorted by over-depletion of the IR beam.

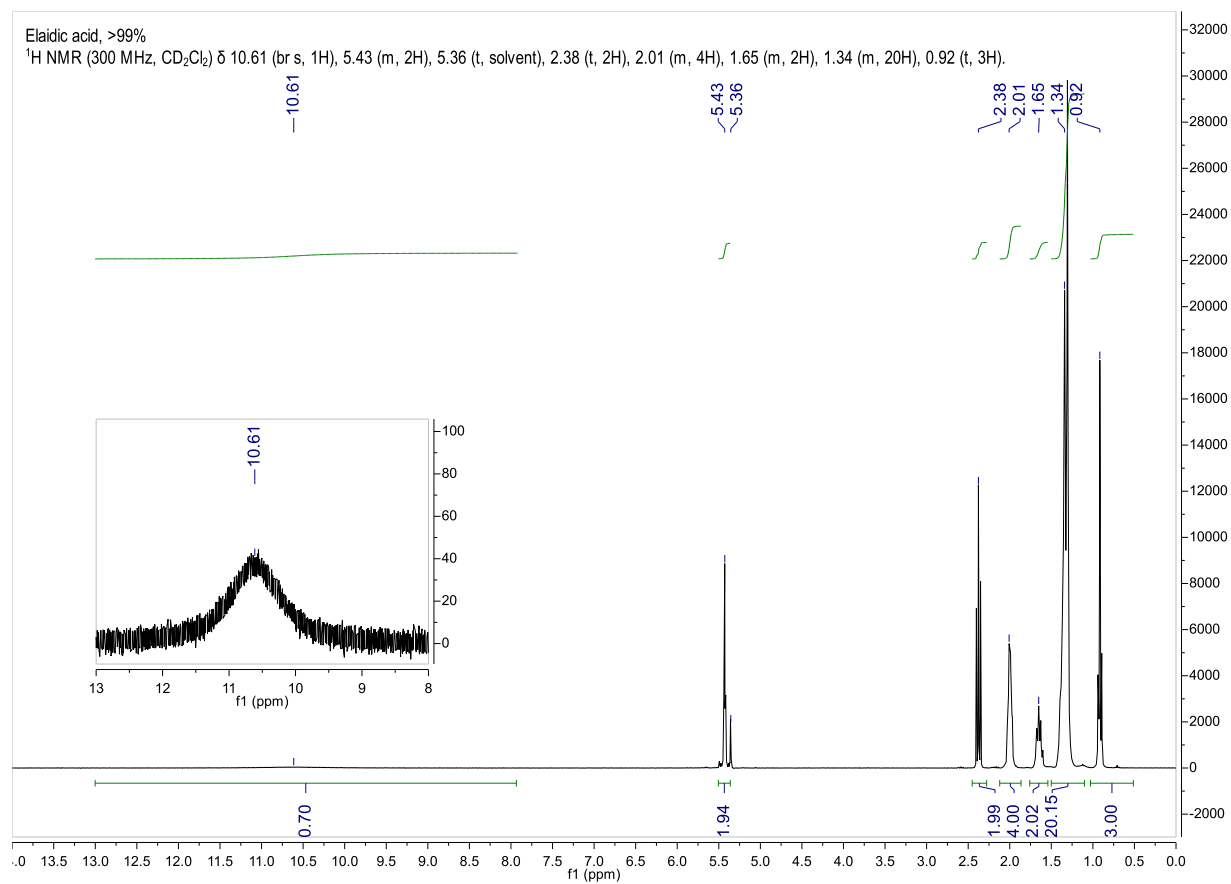
14) ^1H NMR spectra

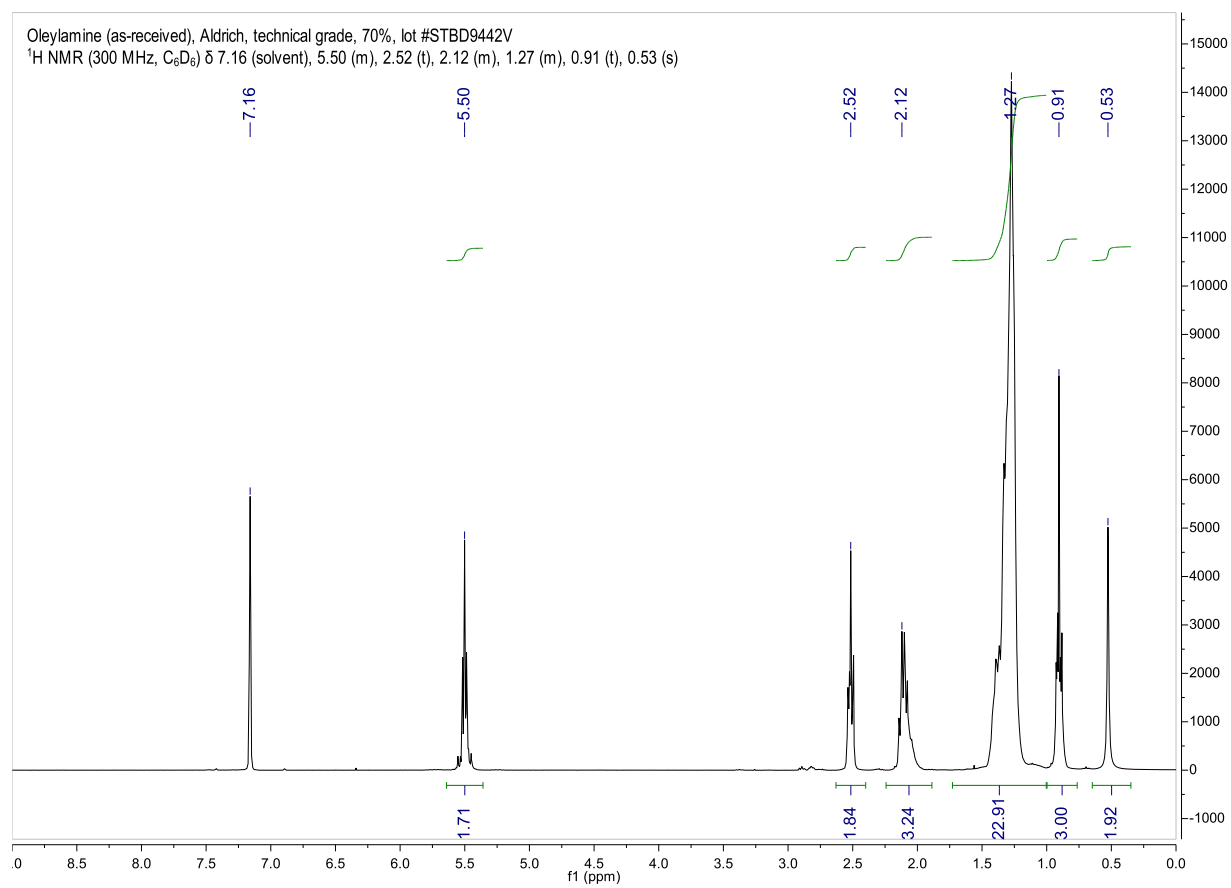


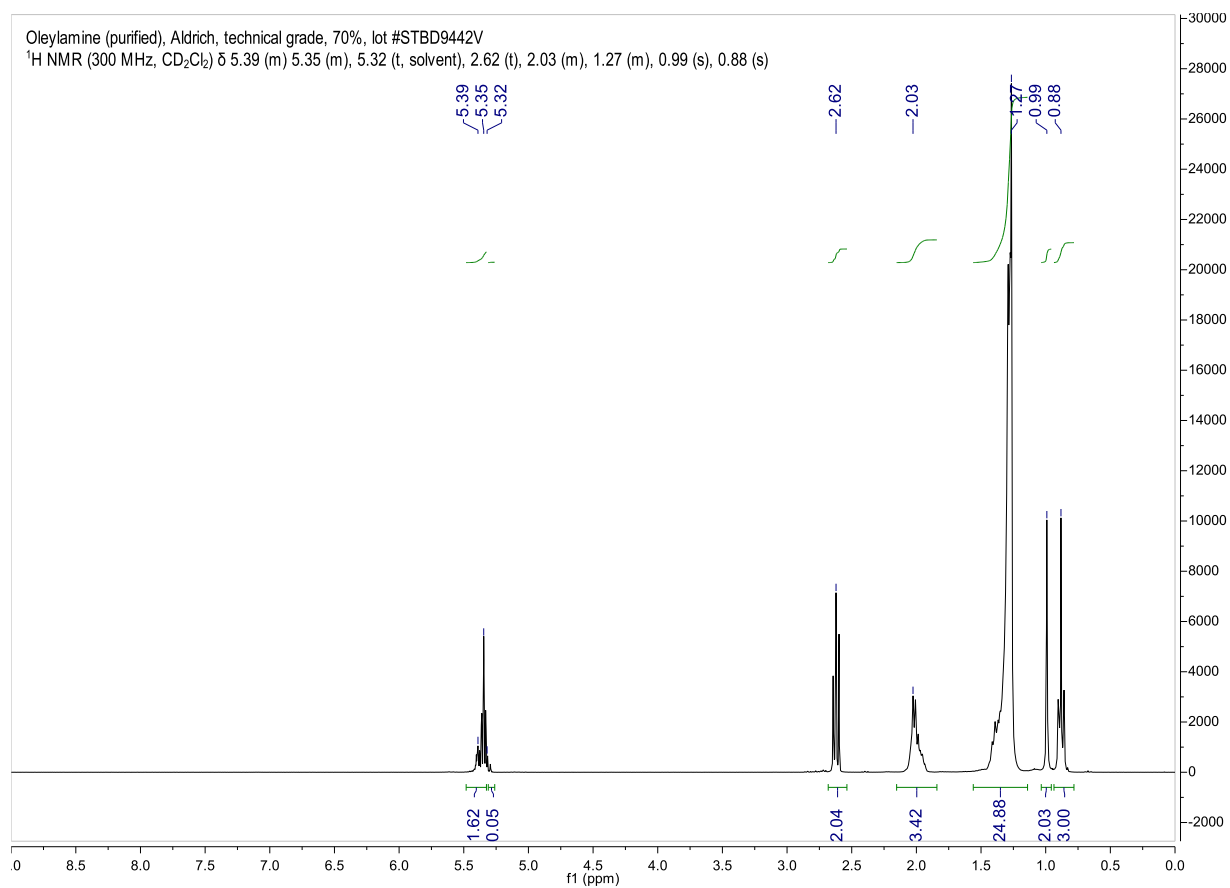


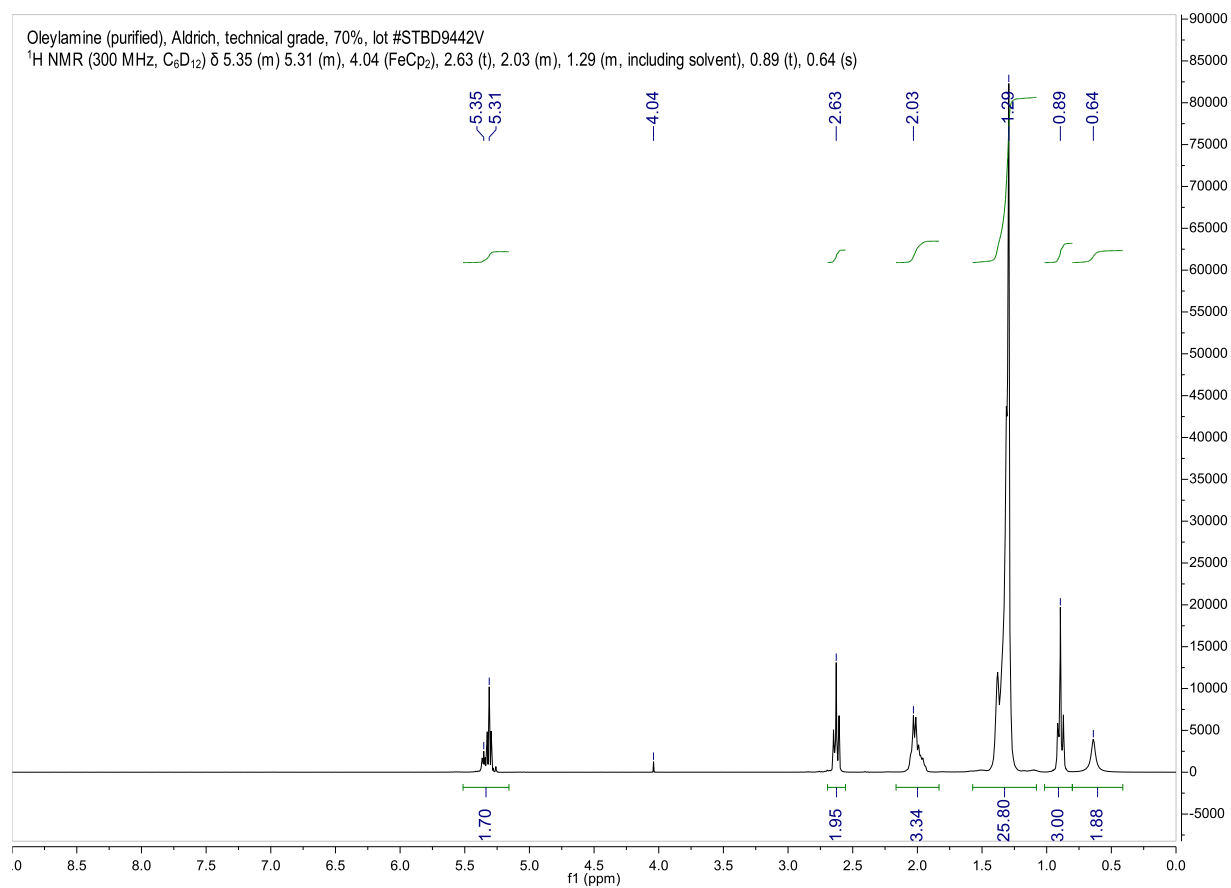


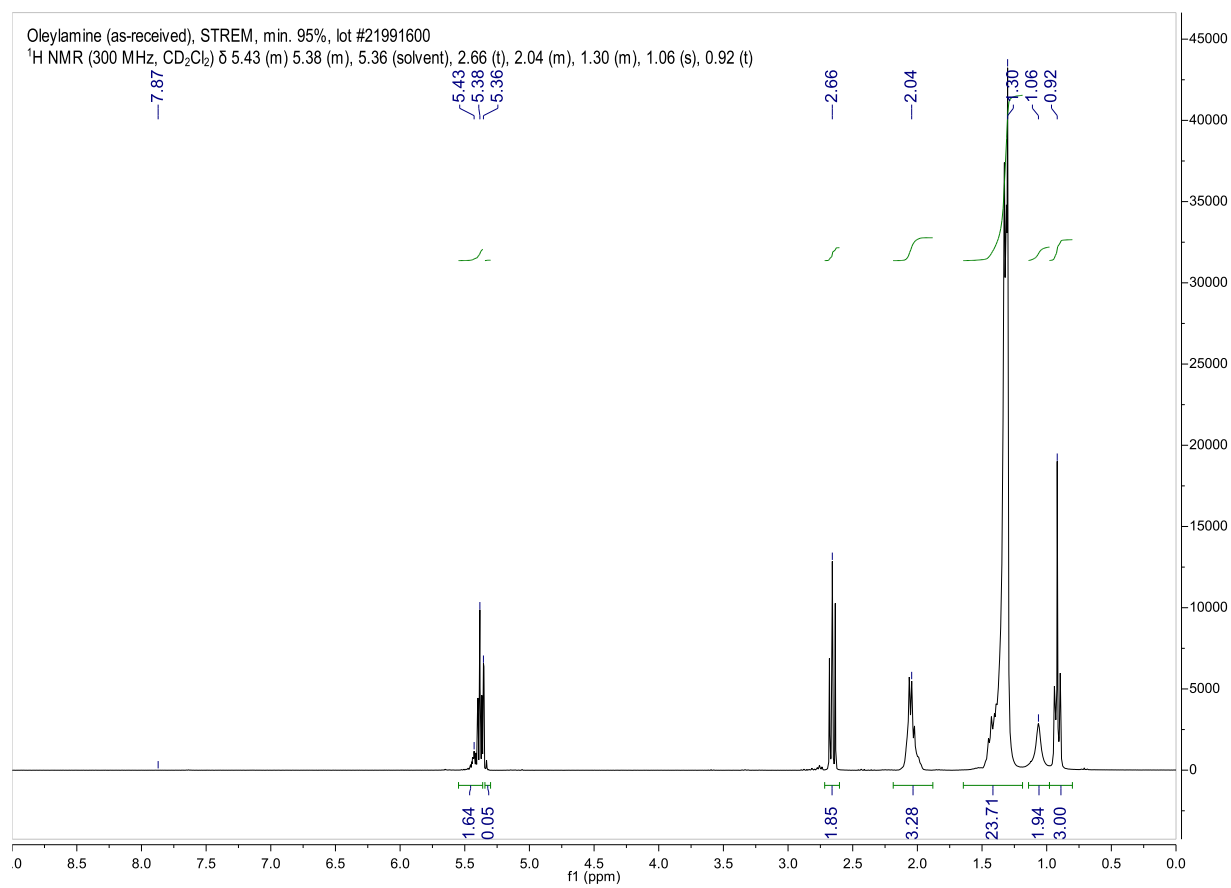


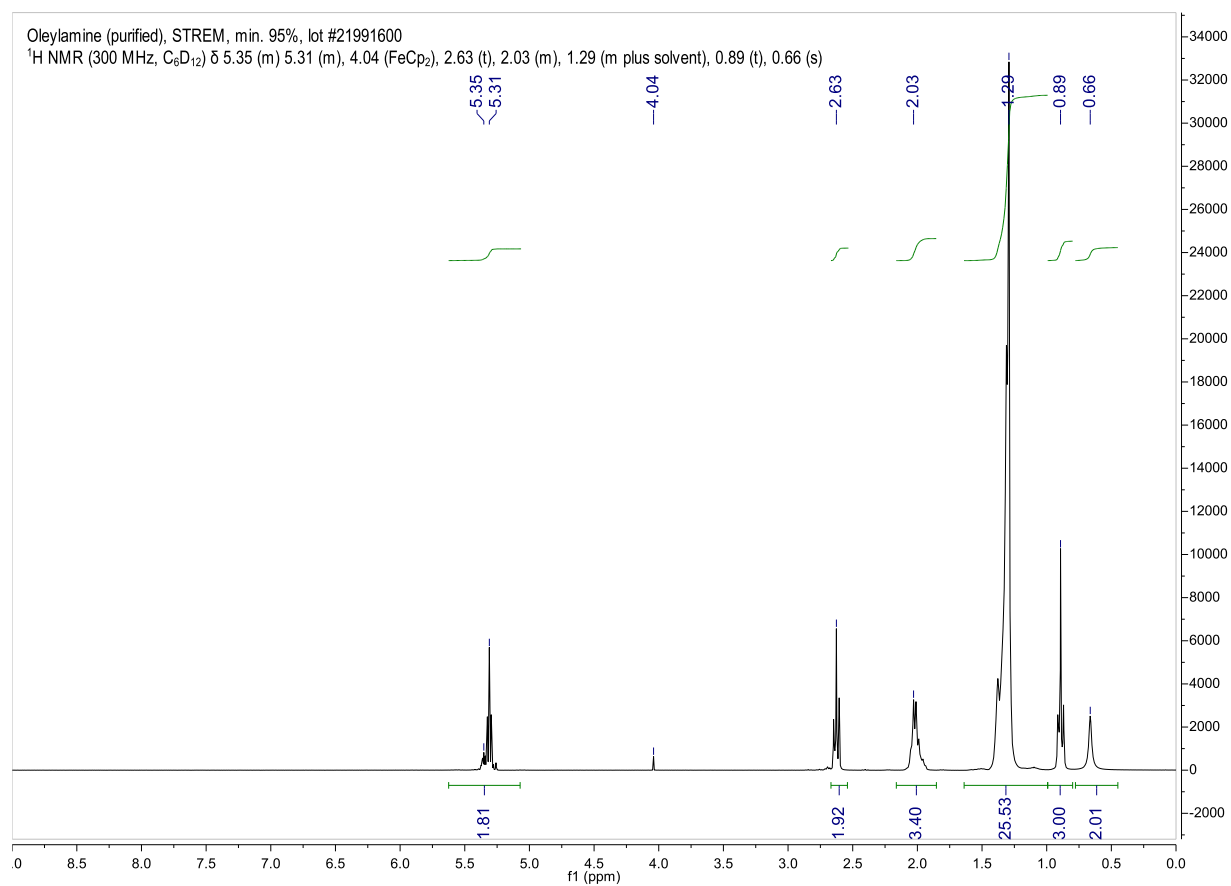


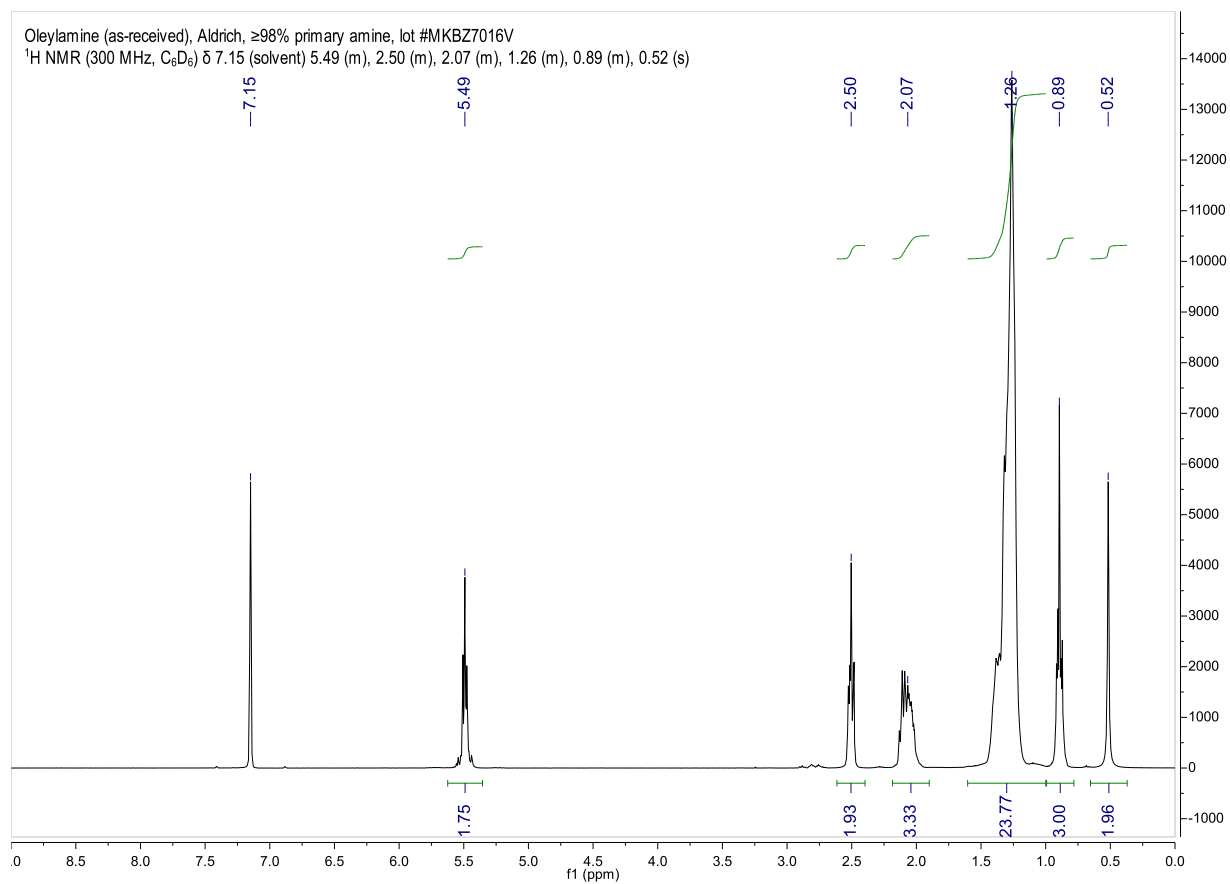


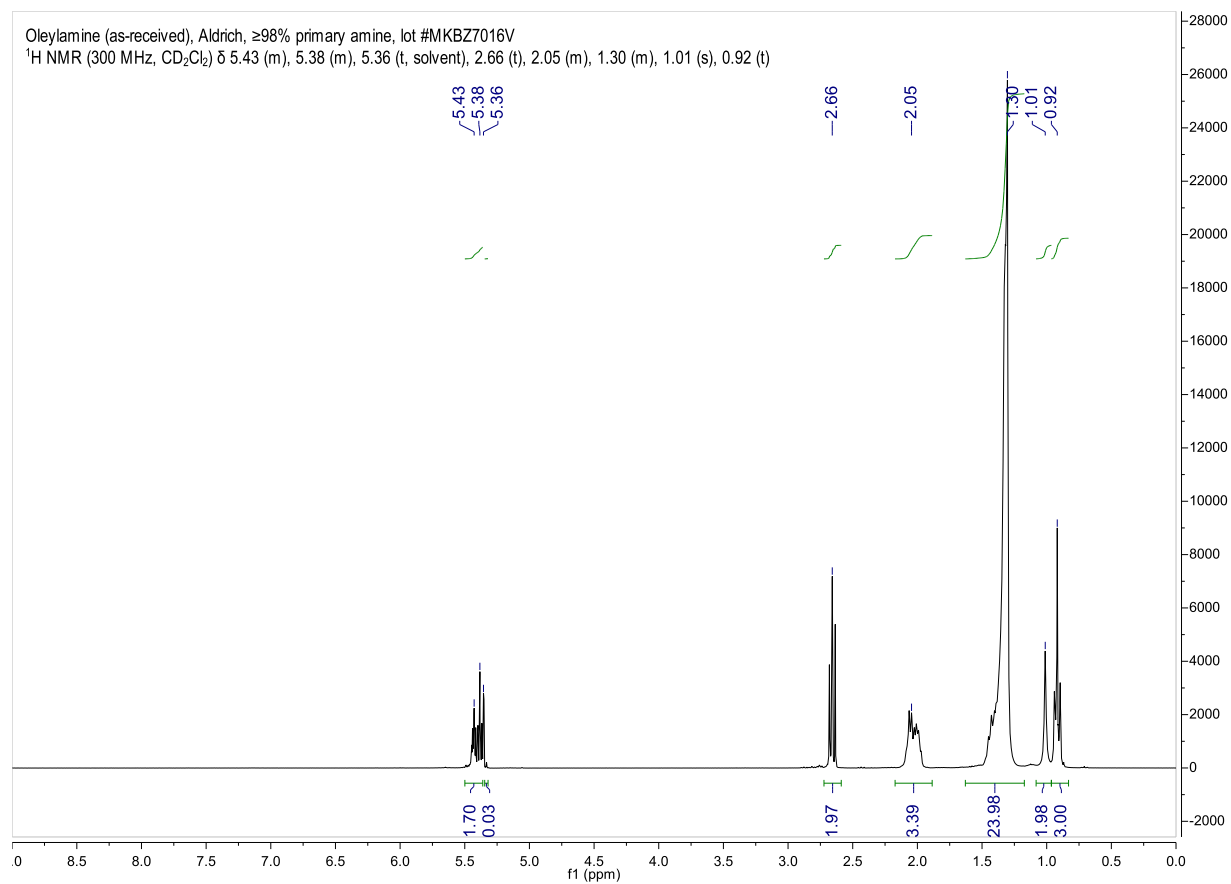


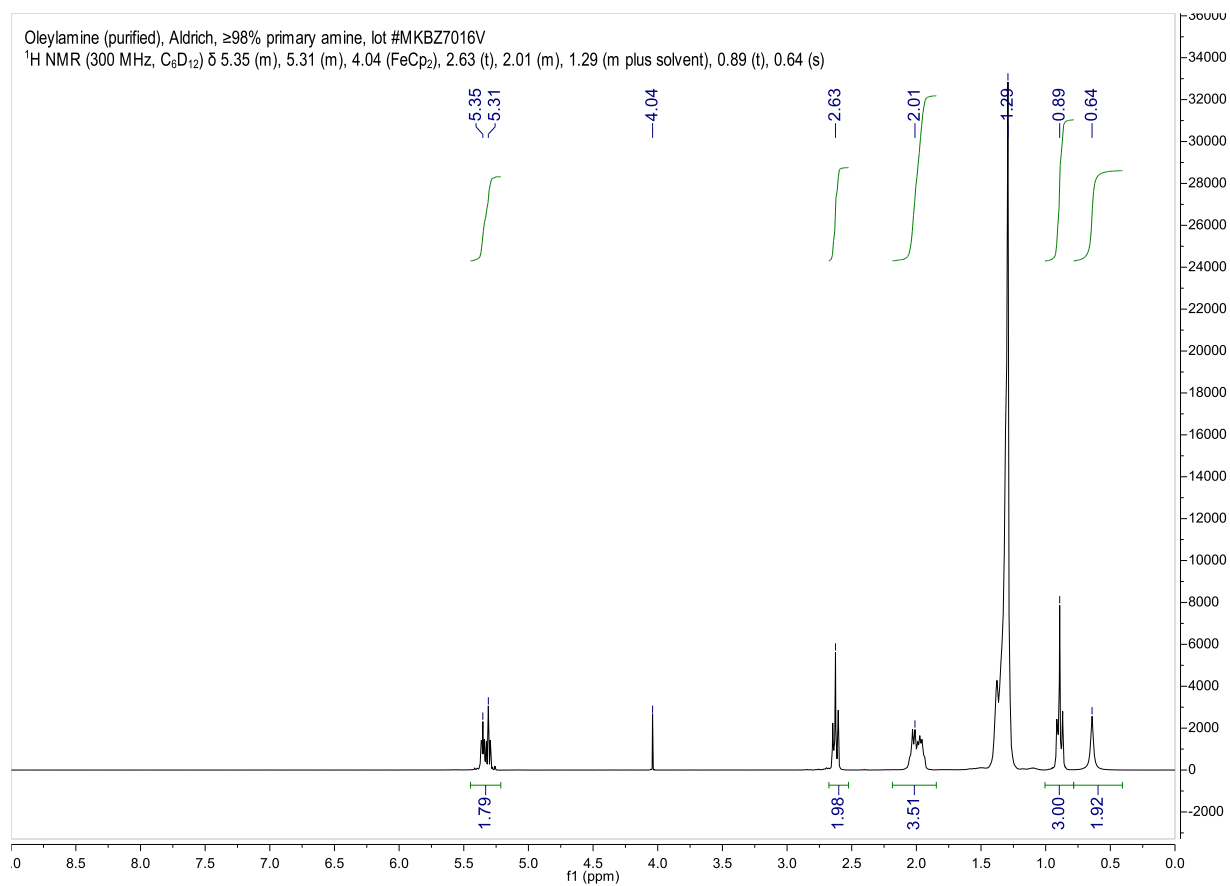


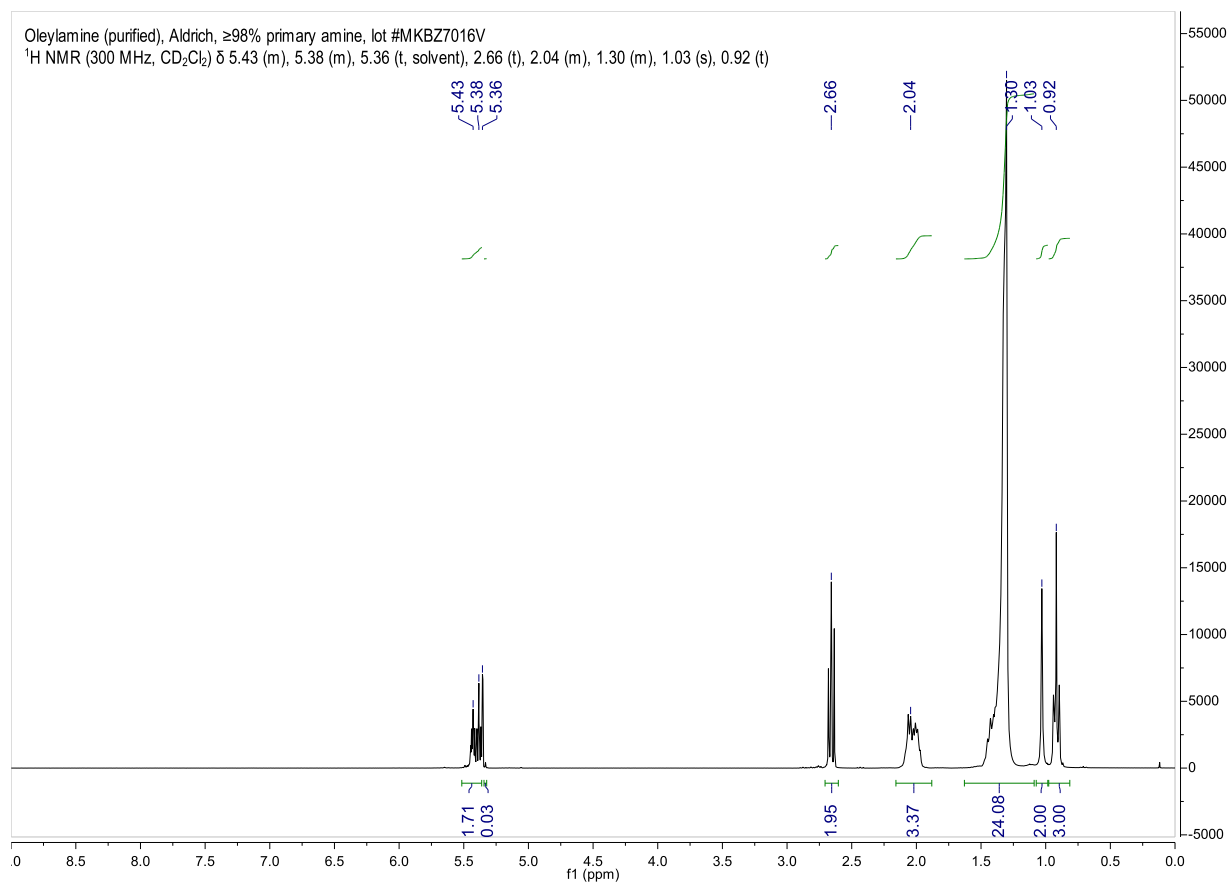


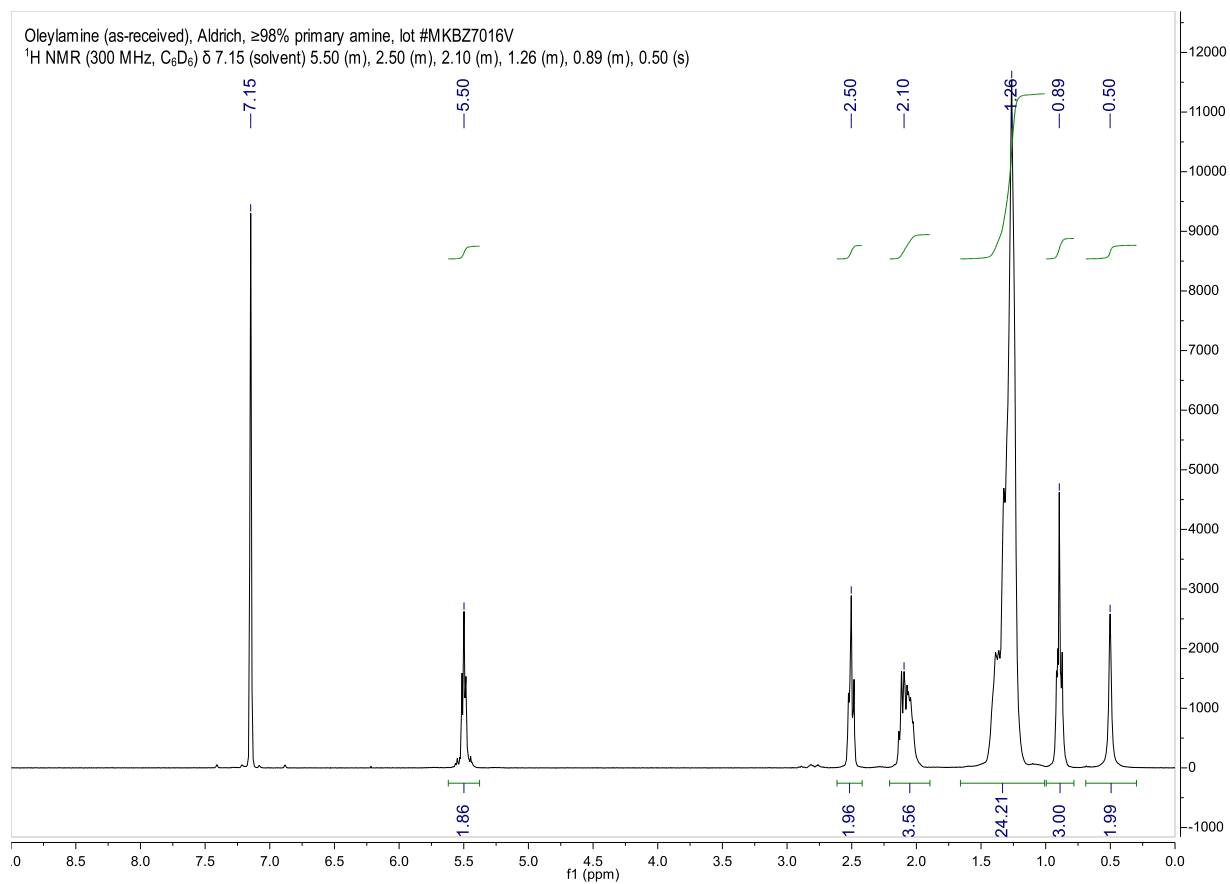












15) References

1. Mohrig, J. R.; Hammond, C. N.; Schatz, P. F., *Techniques in organic chemistry : miniscale, standard taper microscale, and Williamson microscale*. 3rd ed.; W.H. Freeman: New York, 2010; p xvi, 463 p.
2. Fulmer, G. R.; Miller, A. J. M.; Sherden, N. H.; Gottlieb, H. E.; Nudelman, A.; Stoltz, B. M.; Bercaw, J. E.; Goldberg, K. I., NMR Chemical Shifts of Trace Impurities: Common Laboratory Solvents, Organics, and Gases in Deuterated Solvents Relevant to the Organometallic Chemist. *Organometallics* **2010**, 29, (9), 2176-2179.
3. Cademartiri, L.; Bertolotti, J.; Sapienza, R.; Wiersma, D. S.; von Freymann, G.; Ozin, G. A., Multigram scale, solventless, and diffusion-controlled route to highly monodisperse PbS nanocrystals. *J. Phys. Chem. B* **2006**, 110, (2), 671-673.
4. Phillips, L.; Separovic, F.; Aroney, M. J., The aromaticity of ferrocene and some derivatives, ruthenocene and dibenzenechromium as determined via ring current assessment and ^{13}C anisotropic contributions to the ^1H NMR shielding. *New J. Chem.* **2003**, 27, (2), 381-386.
5. Reich, H. J. 5-HMR-1 Integration of Proton NMR Spectra. <https://www.chem.wisc.edu/areas/reich/nmr/05-hmr-01-integration.htm> (June 10, 2017),
6. Zhang, J.; Gao, J.; Miller, E. M.; Luther, J. M.; Beard, M. C., Diffusion-Controlled Synthesis of PbS and PbSe Quantum Dots with in Situ Halide Passivation for Quantum Dot Solar Cells. *ACS Nano* **2014**, 8, (1), 614-622.
7. Hoffmann, E. d.; Stroobant, V., *Mass spectrometry : principles and applications*. 3rd ed.; J. Wiley: Chichester, West Sussex, England ; Hoboken, NJ, 2007; p xii, 489 p.
8. Guidelines for Authors. In *Journal of Organic Chemistry*, American Chemical Society: 2017.
9. Lynch, M. An Investigation of Solutions of Sulfur in Oleylamine by Raman Spectroscopy and Their Relation to Lead Sulfide Quantum Dot Synthesis. Undergraduate Honors Thesis, University of Colorado Boulder, Boulder, CO, 2017.
10. Akkerman, Q. A.; Motti, S. G.; Kandada, A. R. S.; Mosconi, E.; D'Innocenzo, V.; Bertoni, G.; Marras, S.; Kamino, B. A.; Miranda, L.; De Angelis, F.; Petrozza, A.; Prato, M.; Manna, L., Solution Synthesis Approach to Colloidal Cesium Lead Halide Perovskite Nanoplatelets with Monolayer-Level Thickness Control. *J. Am. Chem. Soc.* **2016**, 138, (3), 1010-1016.
11. Shinde, O. S.; Funde, A. M.; Kahane, S. V.; Agarwal, M.; Jadkar, S. R.; Mahamuni, S. R.; Dusane, R. O.; Ghaisas, S. V., Construing the interaction between solar cell surface and fatty amine for the room temperature passivation. *Sol. Energy* **2016**, 135, 359-365.

12. Belman, N.; Israelachvili, J. N.; Li, Y.; Safinya, C. R.; Bernstein, J.; Golan, Y., The Temperature-Dependent Structure of Alkylamines and Their Corresponding Alkylammonium-Alkylcarbamates. *J. Am. Chem. Soc.* **2009**, 131, (25), 9107-9113.
13. Belman, N.; Israelachvili, J. N.; Li, Y.; Safinya, C. R.; Bernstein, J.; Golan, Y., Reaction of Alkylamine Surfactants with Carbon Dioxide: Relevance to Nanocrystal Synthesis. *Nano Lett.* **2009**, 9, (5), 2088-2093.
14. Luo, B.; Rossini, J. E.; Gladfelter, W. L., Zinc Oxide Nanocrystals Stabilized by Alkylammonium Alkylcarbamates. *Langmuir* **2009**, 25, (22), 13133-13141.
15. Tumuluri, U.; Isenberg, M.; Tan, C.-S.; Chuang, S. S. C., In Situ Infrared Study of the Effect of Amine Density on the Nature of Adsorbed CO₂ on Amine-Functionalized Solid Sorbents. *Langmuir* **2014**, 30, (25), 7405-7413.
16. Weidman, M. C.; Beck, M. E.; Hoffman, R. S.; Prins, F.; Tisdale, W. A., Monodisperse, Air-Stable PbS Nanocrystals via Precursor Stoichiometry Control. *ACS Nano* **2014**, 8, (6), 6363-6371.
17. Curtis, A. C. Chemical Education Study on the Effect of Reform of a General Chemistry Course for Majors on Students' Critical Thinking & Femtosecond Spectroscopic Study of Electronic Dynamics in Lead Sulfide Quantum Dots. Doctoral Dissertation, University of Colorado Boulder, Boulder, CO, 2018.
18. Moreels, I.; Justo, Y.; De Geyter, B.; Haestraete, K.; Martins, J. C.; Hens, Z., Size-tunable, bright, and stable PbS quantum dots: a surface chemistry study. *ACS Nano* **2011**, 5, (3), 2004-2012.
19. Fogarty, M. P.; Warner, I. M., Ratio method for fluorescence spectral deconvolution. *Anal. Chem.* **1981**, 53, (2), 259-265.
20. Hirschfeld, T., Computer resolution of infrared spectra of unknown mixtures. *Anal. Chem.* **1976**, 48, (4), 721-723.
21. Volkov, V. V., Separation of Additive Mixture Spectra by a Self-Modeling Method. *Appl. Spectrosc.* **1996**, 50, (3), 320-326.